Short-term scheduling of a combined natural gas and electric power system with wind energy

by

Dan Hu

A thesis submitted to the graduate faculty

in partial fulfillment of the requirements for the degree of

MASTER OF SCIENCE

Major: Industrial Engineering

Program of Study Committee:
Sarah M. Ryan, Major Professor
Lizhi Wang
Peng Wei

Iowa State University

Ames, Iowa

2015

DEDICATION

I dedicate my thesis work to my beloved parents.

TABLE OF CONTENTS

LIST OF FIGURES

LIST OF TABLES

NOMENCLATURE

AC	Alternating Current
Bcf	Billion cubic feet
CCGP	Combined Cycle Gas Plants
DC	Direct Current
DWPF	Day-ahead Wind Power Forecast
DWPFE	Day-ahead Wind Power Forecast Error
EIA	Energy Information Administration
FERC	Federal Energy Regulatory Commission
GENCO	Generation Company
ISO	Independent System Operator
KWh	Kilowatt-hours
kcf	Thousand cubic feet
LNG	Liquefied Natural Gases
LSE	Load Serving Entity
MBtu	Million British thermal units
Mcf	Million cubic feet
MILP	Mixed Integer Linear Programming

MINLP   Mixed Integer Nonlinear Programming

NERC   North American Electric Reliability Corporation

PDE   Partial Differential Equation

p.u.   Per unit

SOS Type2   Special Ordered Set of Type Two

Tcf   Trillion cubic feet

U.S.   United States

ACKNOWLEDGMENTS

I am grateful to my parents, advisor, committee members, professors and friends at Iowa State University. First and foremost, I would like to express my sincere gratitude to my advisor, Dr. Sarah Ryan, for her guidance, patience and support throughout my graduate study. I benefit a lot from her insights, immense knowledge, meticulous and rigorous scholarship. I would also like to thank my committee members, Drs. Lizhi Wang and Peng Wei, for their efforts and contributions to this research. In addition, I am grateful to all course instructors for their insightful teaching and to all my colleagues and friends for providing suggestions and help.

ABSTRACT

The combined natural gas and electricity system with wind energy is one of the most promising models to reduce cost and improve energy efficiency. Wind energy is clean notwithstanding its high uncertainty. Natural gas power generation is also known to be sustainable, cost-effective and fast-response. It plays a significant role in the electricity system and can be used to compensate for wind energy deficiency. Thus, a combined natural gas and electricity system with wind energy is studied to learn how the natural gas fueled power generators can help to incorporate the wind energy in the power system.

The thesis takes the viewpoint of the operator of a combined electricity and gas system, whose goal is to minimize the total operating cost, generating cost and non-served energy cost of the combined system, while satisfying all the operational and equilibrium constraints of each element of the gas system and the electricity system. For simplicity, we assume gas and wind are the only sources of electricity. A mixed integer nonlinear optimization model is formulated to investigate the hourly unit commitment and dispatch solution for the electricity system as well as the natural gas system's hourly working schedule in a single day. Additional linear constraints are formulated with binary variables to approximate the nonlinear constraints of gas flow in natural gas pipelines, and the resulting mixed integer linear optimization model can be solved efficiently to optimality. In addition, a two-stage stochastic optimization model is applied to incorporate the uncertainty of wind power production and learn the operational decisions of pipelines, gas supply, and generating unit commitment in the first stage. In the second stage, decisions on the hourly schedule of gas-fueled power generators, power flows and the gas storage flows are made given various wind energy scenarios.

The computational results of a deterministic model with fixed reserve constraints and the here and now (stochastic optimization) model are compared, along with a wait and see model that gives a lower bound on the expected cost of the stochastic optimization model. In the deterministic optimization model with reserves, the planning problem is solved in the day-ahead market in view of the wind energy forecast and the first-stage variables are fixed to those optimal values. Then, in the real time market, under various scenarios for actual wind energy supply, a dispatch model without reserves is solved to test how well those day-ahead decisions perform. The numerical results for a small test case illustrate that the gas fueled power generators and gas storage are able to counteract the wind energy deficiency to satisfy demand at a lower and more stable cost by incorporating various wind energy scenarios in the stochastic optimization model.

CHAPTER 1. OVERVIEW

1.1 Introduction

An electric power system is a network of electrical components used to supply, transmit and deliver electric power, which is composed by generators that supply the power, the transmission system that transmits electric power from the generating units to the load centers and the load serving entities' (LSEs') distribution system that feeds the power to nearby homes and industries. According to the Energy Information Administration's (EIA's) Annual Energy Outlook 2014 forecast, the electricity demand in the U.S. will increase by 0.9% per year from 3,826 billion kilowatt-hours (KWh) in 2012 to 4,954 billion KWh in 2040 (EIA, 2014). The increasing electricity consumption becomes more dependent on the adequacy of the electric power system due to the further development of industry and the improvement in quality of life. An unstable electric power system will cause enormous economic loss and chaos. Therefore keeping a stable and reliable electric power system is of great importance.

The major factors influencing the stability and reliability of the electric power system are fuel options, technologies and operations of the generating units, transmission and distribution system. When current fuel options and technologies are limited, establishing a short-term model is essential for a reliable electric power system to operate the electric power and gas systems simultaneously. On the fuel and generator technologies aspect, the EIA predicts that the share of natural gas in the total electric power generation will rise from 27% in 2012 to 31% in 2040, while the coal-fired generators' corresponding share will decrease from 39% to 34%. This increase of the gas fueled generators' share originates from the retirement of coal-fired

generators, development of high efficiency natural gas fueled generators, the increase of natural gas supply, with a relatively stable gas price since 2009, and potential emission regulations. Hence, for the sake of maintaining a stable and reliable electric power system, more research about how to make unit commitment and dispatch decisions for those gas fueled power generators is requisite.

Wind energy, with the cheapest operational cost, could be added into the power transmission grid directly and thus relieve the pressure on those gas fueled power generators. Due to the pre-schedule scheme of natural gas system and electric power system, one day ahead of the actual operating day, a decision about how much gas must be extracted in the gas wells is required to be made on the basis of wind turbine output prediction. However, there is a discrepancy between the forecast and actual value of wind turbine output. Knowing how to operate this combined natural gas and electric power system with wind energy included is crucial.

1.2 Problem Statement

In this thesis, we consider short-term scheduling of a combined power and natural gas system with wind power included. One day ahead of the actual operating day, the combined system's operator is supposed to make a decision about in which hour to start up or shut down which natural gas fueled power plant for the power system and daily gas production in gas wells, pressure in each gas node, gas flow amount and direction in each gas pipeline and the compressors' working schedule for the natural gas system. Then in the real time gas and power markets, the dispatch solution of the power system, corresponding non-served gas and power, non-served gas and power in each node, power transmission amounts in transmission lines, storage flows and storage levels of gas storage facilities will be determined.

On the model formulation aspect, owing to the uncertainty of wind power output, we formulate both a deterministic optimization model with fixed reserve constraints which is the traditional approach applied in the power system and a two-stage stochastic optimization model to minimize the total expected cost for 24 successive hours. For the two-stage stochastic optimization model, with the prescribed non-electric gas demand and electric demand prediction, we find the optimal solutions given various wind energy scenarios, while the first stage solution is the same for each scenario. Also, we solve the deterministic optimization problem with forecasted hourly wind energy and mandated reserves, and then fix all those variables in the first stage and obtain the optimal solutions to those variables in the second stage given various wind energy scenarios. Then we compare the total cost of these two models to see if employing the two-stage stochastic optimization model could decrease the total cost of the combined system.

1.3 Thesis Structure

Including this introduction chapter, this thesis is organized into seven chapters. Chapter 2 presents a comprehensive literature review on the integrated power and gas systems as well as wind energy scenario generation methodologies. Chapters 3 and 4 introduce the components and general modeling methodologies of the natural gas system and the power system, respectively. Chapter 5 further discusses the details of the deterministic mixed integer nonlinear optimization model, the deterministic mixed integer linear optimization model and the two-stage stochastic optimization model of the combined system as well as the model assumptions and notations. In Chapter 6, one day-ahead hourly wind energy scenarios are described and a simple case study is made to compare the results of the deterministic model with those of the stochastic model. In

Chapter 7, a comprehensive summary of this thesis is made and future research regarding the

natural gas system modeling, uncertainties, constraints and methodologies is discussed.

CHAPTER 2. LITERATURE REVIEW

2.1 Combined Power and Natural Gas System Model Methodologies

Many researchers have discussed approaches to modeling the combined natural gas and power system. The effect of natural gas infrastructure and gas unit price on power generation scheduling is addressed by using security-constrained unit commitment (Shahidehpour et al., 2005). Using characteristic disruption scenarios and taking the cascading effects of integrated power and gas system disruptions into account prove the efficiency and effectiveness of the integrated system (Urbina and Li, 2007). Dual decomposition, Lagrangian relaxation and dynamic programming are used to solve a large scale mixed-integer nonlinear integrated electricity-gas optimal short-term planning and unit commitment problems with hydrothermal system included (Unsihuay et al., 2007). A day-ahead integrated model incorporating the natural gas network constraints into the optimal solution of security-constrained unit commitment and fuel diversity is applied as an effective peak shaving strategy (Li et al., 2008). Benders decomposition is applied in the security-constrained unit commitment problem with natural gas transmission constraints (Liu et al., 2009). A coordination scheme for electric power and natural gas infrastructure is proposed in which a bi-level problem is formulated to investigate the combined system (Liu et al., 2011). The upper level problem is the electric power system including the unit commitment and dispatch problem, while the lower level problem concerns the natural gas system.

Recently, more research studies focus on the stochastic aspect of the natural gas system and the electric power system. In 2013, Correa-Posada and Sánchez-Martín proposed a two-stage stochastic optimization model of the unit commitment with natural gas constraints for the

analysis of infrastructure outages, in which the first stage optimizes the commitment and production decisions and all the other derivative variables are computed in the second stage (Correa-Posada and Sánchez-Martín 2013). In 2014, Correa-Posada and Sánchez-Martín applied linear sensitivity factors to perform security analysis and adjust decisions in advance to assure the total system remains stable even when a single contingency happens (Correa-Posada and Sánchez-Martín 2014c). None of the previous research studies included the renewable energy uncertainty.

Several papers discuss how to model the gas flows in pipelines. For the most general case of transient flow, the laws of conservation of mass, energy and momentum are applied to find three partial differential equations (PDEs) (Osiadacz, 1987). However, although the gas state condition could be added to those three PDEs to help identify the closed form of solution, more equations are required due to the large number of variables in the transient model. Thorley and Tiley reviewed the theoretical and some experimental results of the unsteady and transient flow of compressible fluids in pipelines (Thorley and Tiley, 1987). Given the special physical characteristics of gas pipelines, a unidirectional flow model was proposed and various derivative models of different thermal conditions were developed. A one-dimensional, non-isothermal gas flow model was solved to simulate the slow and fast fluid transients and address the effect of various thermal models on the flow rate, pressure and temperature in the pipelines (Chaczykowski, 2010). Given a one dimensional homo-thermal steady state flow condition, those partial differential equations for transient state flow could be simplified and the Weymouth equation was proposed to model gas flow in passive pipelines (Liu et al., 2011).

On the nonlinearities' approximation aspect, there are several piecewise methods to approximate the Weymouth equation in the gas system. A theoretical and computational

comparison of piecewise linear models for the gas flow in the pipelines is made in which Correa-Posada and Sánchez-Martín (2014a) compared aggregated convex combination models including a special ordered set of type two (SOS Type2) model, a basic convex combination model and logarithmic model, desegregated convex combination models composed of desegregated convex combination model and logarithmic desegregated convex combination model, as well as multiple choice model and incremental model. The computation result declares that the incremental method is the fastest method given linearization of flow squared and in- and outlet pressure squared.

2.2 Wind Energy Scenario Generation Methodologies

Unit commitment and dispatch problems are traditionally based on fixed reserve limits. With the power turbine technologies' development, the capacity of wind turbines has increased significantly and wind power has become an important energy resource. Thus the methodologies of combining wind power outputs into the regular power system attract more researchers' attention. Scenario generation is often involved because of the high uncertainty associated with wind energy. Many research studies have been done to address scenario generation problem (Kaut and Wallace, 2007). One approach is to deal with the specified marginal distribution and correlation matrix directly (Lurie and Goldberg, 1998). Another commonly used method is finding the discrete scenario distribution with the minimum pertaining approximation error (Pflug, 2001). In 2001, Høyland and Wallace proposed an approach of approximating multiple random variables simultaneously by minimizing the error of a set of statistical specifications (e.g., mean, variance, skewness, etc.) (Høyland and Wallace, 2001). Specifically for wind energy, Barth applies Monte Carlo simulations and first-order autoregressive time-series model

with noise to generate wind scenarios (Barth et al., 2006). An approach combing quantile regression with a Gaussian copula is demonstrated to be valid (Pinson et al., 2009).

2.3 Summary and Research Gap

Although many research studies have been done in the scheduling problem on the combined natural gas and electric power system or unit commitment and dispatch problem with wind included, there has not been a rigorous model combining the unit commitment and dispatch problem including power and gas systems scheduling problem with wind energy. Given various wind energy scenarios, the electric power system is required to adjust its decision variables fast and accurately, and the gas fueled power plant can compensate for the discrepancy between wind forecast and actual wind power supply. In this thesis, we propose a combined natural gas and electric power system including wind energy to address how the natural gas system could help to address the non-determinacy of wind power output in the electric power system.

CHAPTER 3. NATURAL GAS SYSTEM

3.1 Introduction to the Natural Gas System

Natural gas is a hydrocarbon gas mixture formed mainly by methane, but commonly contains some other higher alkanes and carbon dioxide, nitrogen and hydrogen sulfide. Natural gas is divided into dry and wet natural gas on the ground of the composition and utility purpose. Dry natural gas is the remaining part after removing all the liquefied hydrocarbons (hexane, octane, etc.) and non-hydrocarbon (helium, nitrogen, etc.), and methane is almost the only component of dry natural gas. Wet natural gas contains no more than 85% methane and has a higher percentage of liquid natural gases (LNG) including butane and ethane. While the five largest dry gas-producing states are Texas, New Mexico, Louisiana, Oklahoma and Wyoming, the five highest-yielding wet gas states include Pennsylvania, Texas, Louisiana, Oklahoma and Colorado. Furthermore, dry gas is normally used in heating and cooling systems and for electric power generation. The world's first industrial extraction of natural gas began at Fredonia, New York, USA in 1825. After almost 200 years of development, an integrated and organized natural gas system, made up by supplies, transmission and distribution network and storage facilities, is established (EIA, 2014b). Figure 1 illustrates an integrated natural gas industry network.
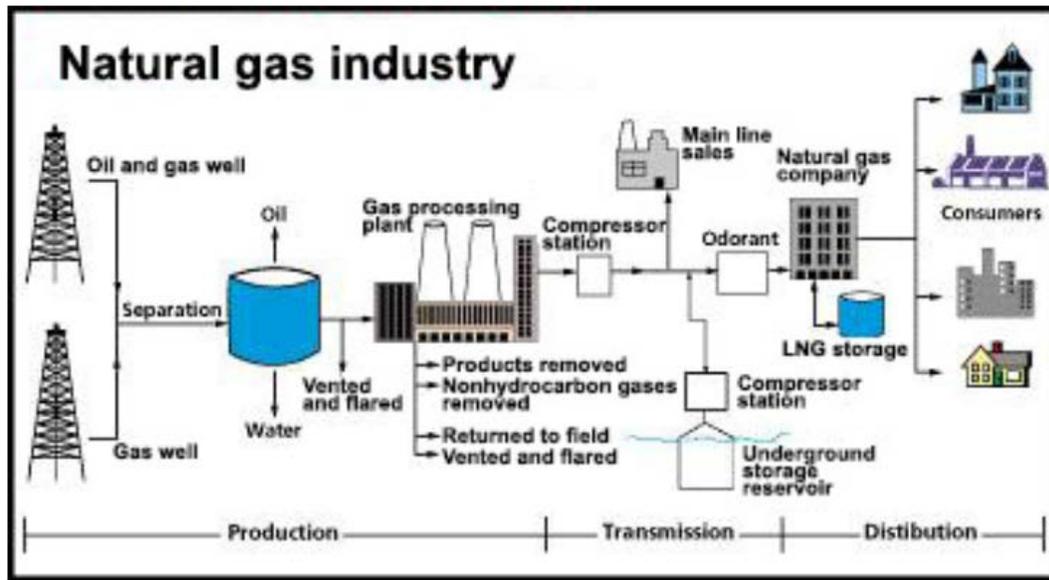
Figure 1 Natural gas transmission networks (DTE Energy, 2015)

3.1.1 Supplies

The world's largest gas field is the offshore South pars/ North dome gas-condensate field, shared between Iran and Qatar with verified reserves of 51 trillion cubic meters (Tcf) of natural gas and 50 billion barrels of natural gas condensates. For the U.S., proved reserves of total natural gas (including natural gas plant liquids) increased 2% per year on average since 1983 and especially increased by 9.7% (31.3 Tcf) in 2013. They reached a record high for the U.S. of 354 trillion cubic feet (Tcf), driven principally by shale gas developments (Figure 2). In 2012 the total natural gas proved reserves had a large drop due to the relatively low natural gas price which was lower than $2 per MBtu in April 2012 (EIA 2014b).
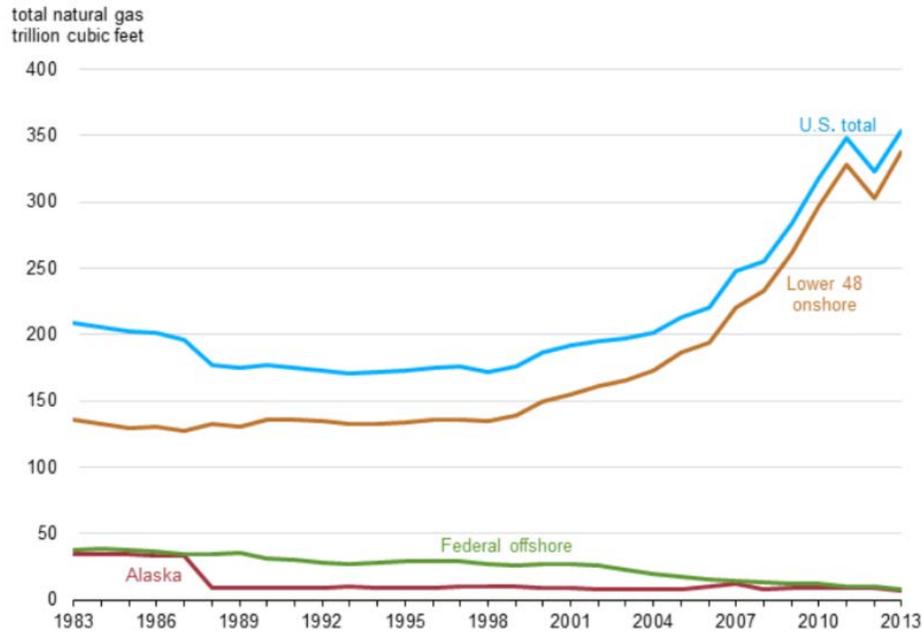
Figure 2 U.S. total natural gas proved reserve from 1983 to 2013 (EIA, 2014b)

For the annual production of natural gas, the gross withdrawals of natural gas for U.S.

reaches 3000 billion cubic feet (Bcf) among which Texas takes account of 27 percent at 821 Bcf,

while Pennsylvania and Alaska take account of 10 percent at 326 Bcf and 322 Bcf respectively.

From Figure 3, we can tell that PA, WV, WY, CO, NM, TX, OK, AR, LA and Gulf of Mexico

are the major producing area of natural gas. Nationwide, dry natural gas production in the U.S.

increased by 35% from 2005 to 2013, with the natural gas share of total U.S. energy

consumption rising from 23% to 28%. Lower 48 shale gas production (including natural gas

from tight oil formations) is predicted to increase by 73% in the reference case, from 11.3 Tcf in

2013 to 19.6 Tcf in 2040, leading to a 45% increase in nationwide U.S. dry natural gas

production, from 24.4 Tcf in 2013 to 35.5 Tcf in 2040. Growth in tight gas, federal offshore, and

onshore Alaska production also contribute to overall production growth over the projection

period. In summary, with the recent annual production and reservoir amount, the natural gas

could be utilized for another 80 to 100 years (EIA 2015a, b).
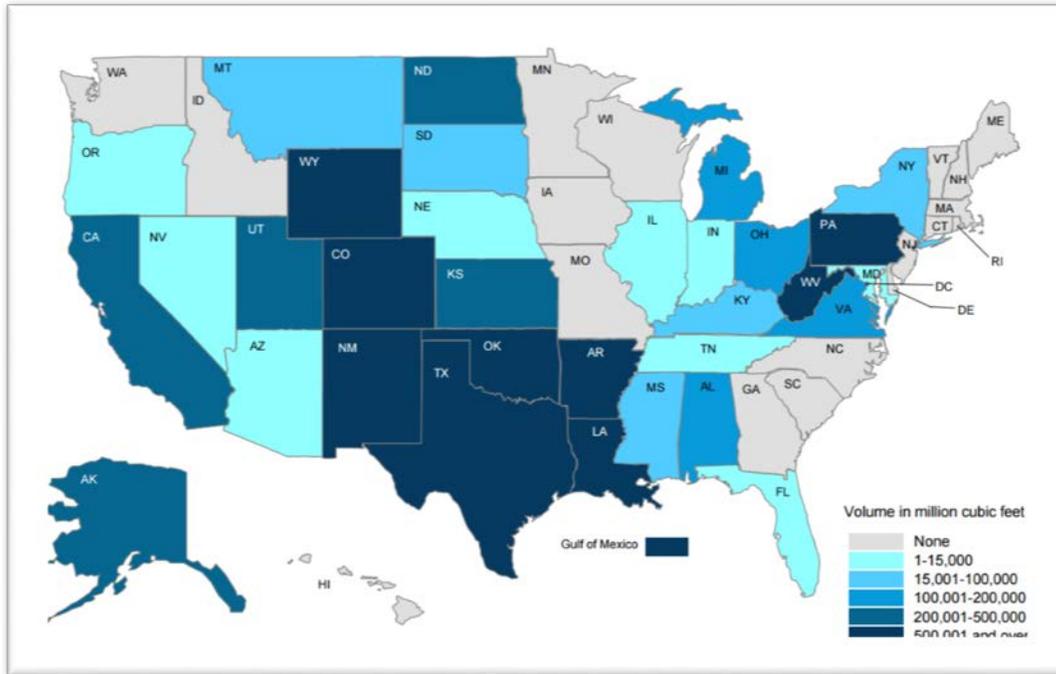
Figure 3 Marked production of natural gas in the U.S. & Gulf of Mexico 2013 (EIA, 2015b)

3.1.2 Transmission

In the light of various natural gas characteristics and transmission situations, the natural gas transmission network is normally divided into natural gas pipeline transmission and liquefied natural gas transportation.

Liquefied natural gas (LNG) is natural gas cooled to about -260°F for shipment and storage as a liquid whose volume is about 600 times smaller than in its gaseous form. With such a compact form, natural gas can be shipped in special tankers from producing areas to terminals in the United States to other countries and provides a way to move it long distances where pipeline transport is not feasible. At these terminals, the LNG is extracted to a gaseous form and transported by pipeline to distribution center, industrial customers and power plants. In 2013, the gross U.S. dry natural gas production was equal to 93% of U.S. natural gas consumption, while

net natural gas imports contributed to the remaining consumption volume and LNG imports

contributed about 0.4% of total natural gas consumption in 2013. LNG imports from Norway,

Qatar, Trinidad and Tobago, and Yemen contributed about 97% of total LNG imports (EIA,

2015b).

The U.S. natural gas pipeline network is a highly integrated grid made up of about 1.5

million miles of mainline and other pipelines that link production areas and natural gas markets.

It can move natural gas to about 72 million customers in any location and delivered 24 trillion

cubic feet (Tcf) natural gases in 2012 in the continental United States. Natural gas from the

wellhead normally contains contaminants and natural gas liquids, while all those natural gas

pipelines have special requirement of quality measures for natural gas flowing in them.

Consequently, in order to supply uniform quality gas to the pipelines and customers, from the

wellhead to the customers, transporting natural gas needs many infrastructures, physical transfers

and some processing steps which could be classified into three categories of processing,

transportation and storage. First of all, raw natural gas is moved through the small-diameter low-

pressure pipelines named gathering pipelines from the wellheads to the natural gas processing

plant, where several processes are involved to remove oil, water, natural gas liquids, and other

impurities such as sulfur, helium, nitrogen, hydrogen sulfide, and carbon dioxide, or to an

interconnection with a larger mainline pipeline. Secondly the processing plant extracts natural

gas liquids and impurities from the natural gas stream and loads its products to the mainline

transmission systems to transport natural gas from the producing areas to market areas with

wide-diameter, long-distance, high-pressure interstate and intrastate pipelines, in which

compressors stations located at specific location along the pipelines would increase gas pressures

and push them to move in one direction. Thirdly, at the locations where pipeline intersect and

flows are transferred, market hubs balance the natural gas demand and supply. Lastly, the exchanged amount of natural gas will be transferred to the end customers by applying the distribution network with pipe diameters from 2 to 24 inches, small compressors, regulators and block valve stations, and protection and metering equipment (EIA 2014a). Figure 4 illustrates the gas flow capacity in the principal interstate pipelines.
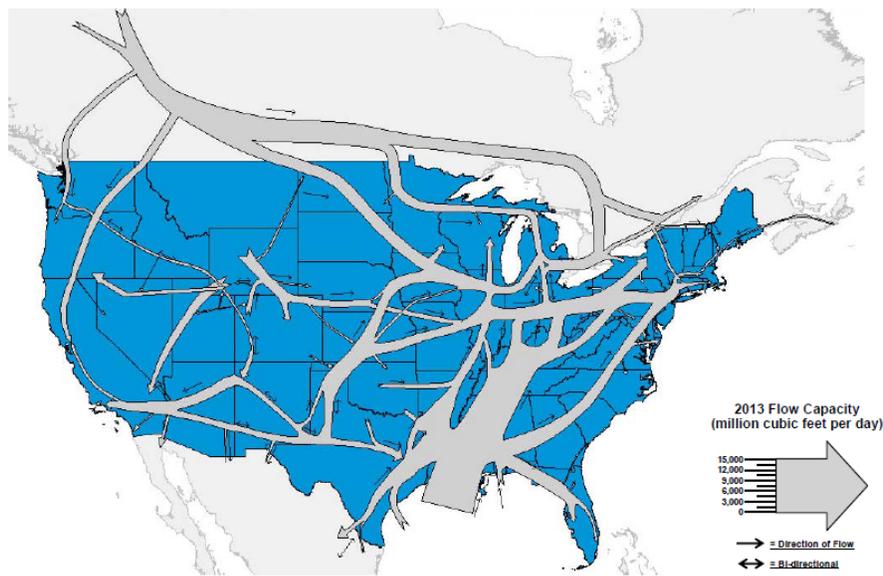
Figure 4 Principal interstate natural gas flow capacity summary 2013 (EIA, 2015b)

3.1.3 Storage

Natural gas storage is introduced to develop natural gas system's stability and reliability. Basically, in view of a larger natural gas supply, the price of natural gas is relatively low and those additional natural gas amounts can be injected into storage facilities to assure the system's equilibrium, whereas the required amount of natural gas is able to be withdrawn from storage facilities given a high natural gas demand and price. The most popular and significant natural gas storage type is underground natural gas storage, among which depleted gas reservoirs, aquifer

reservoirs and salt cavern reservoirs are three primary categories. Figure 5 shows these three

underground natural gas storage categories locational distributions in the U.S.
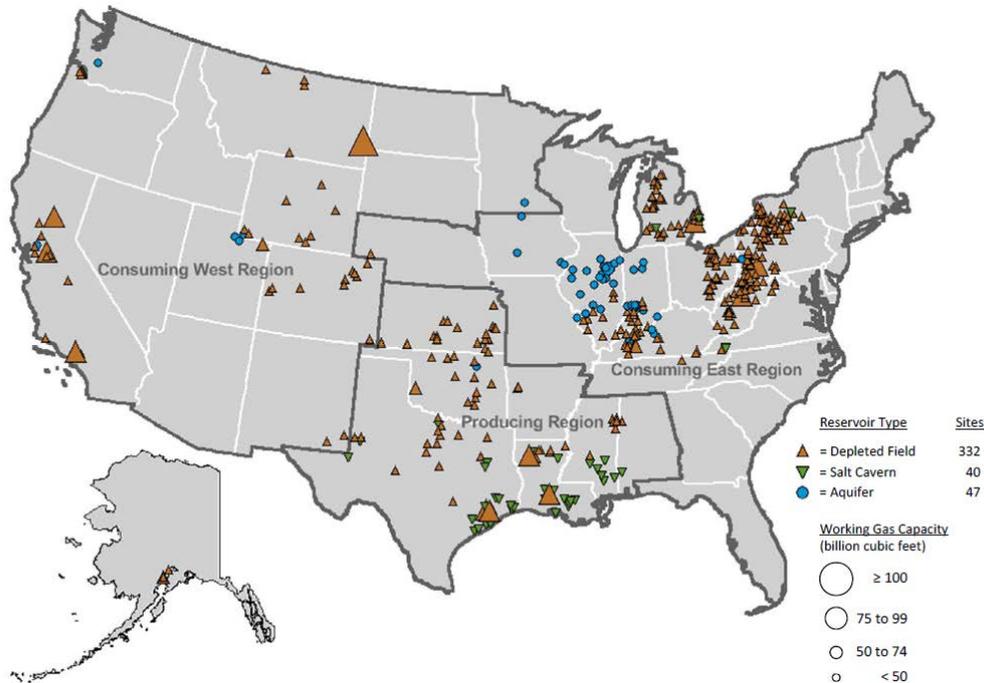
Figure 5 Locations of existing natural gas underground storage fields in the U.S. 2013 (EIA, 2015b)

Each underground storage facility has cushion capacity and working capacity, among which

cushion capacity is used to maintain working pressure in the storage facilities and cannot be used

as production but working capacity could be withdrawn from storage facilities. Depleted gas

reservoirs are the reservoir formations of natural gas fields after producing all their economically

recoverable gases. With the natural storage condition and natural gas and hydrocarbons in them,

depleted gas reservoirs are the most prominent and common underground storage facilities and

do not require the injection of gas that will be physically unrecoverable. Aquifers are rock

formations that are natural underground water reservoirs. Different from depleted gas reservoirs,

extensive investigations need to be done to check the geological and physical characteristics of

those aquifer formations and evaluate their suitability for natural gas storage. With a suitable

aquifer, many processes including wells installation, extraction equipment, pipelines,

dehydration facilities, and possibly compression equipment are required to transform it to a

qualified gas storage facility. Apart from the cost of investigation and installation processes

mentioned above, it is indispensable to inject some gas, up to 80 percent of the total gas volume,

to be physically unrecoverable as cushion gas. Therefore aquifers reservoirs are not only the

most expensive but also time consuming and the least desirable natural gas storage facilities. One

suitable salt feature could be transformed to a salt cavern to store natural gas by the process of

solution mining, which is pumping down a borehole into the salt to dissolve some salt and

extract the water until the cavern reaches the desired size. Meanwhile their cushion requirement

is as low as 33 percent of total gas capacity, lower than depleted gas reservoirs and aquifers. Gas

in salt caverns could be withdrawn and replenished more quickly and readily because their

capacities of are usually much smaller than those of depleted reservoirs and aquifers, whereas the

depleted gas reservoirs and aquifers are scheduled to be replenished once a year (DTE Energy,

2015).

Beyond that, for those areas without underground storage facilities, LNG tanks are also

effective and efficient in storing natural gas. Furthermore, on account of the compressibility of

natural gas, gas is compressed and stored in pipelines. This kind of storage, usually called line

packing storage, is also an efficient way to store natural gas.

3.2 Pipelines Network

3.2.1 Passive pipelines modeling

Transient modeling

Gas flows in pipelines are directly impacted by the pipelines' length, diameter, operating temperature, roughness, the composition of natural gas, altitude change of pipelines and the boundary conditions. In theory applying the laws of conservation of mass, energy and momentum (Osiadacz, 1987; Mohitpour, 2003), gas flows in pipelines are determined by several partial differential equations (PDEs). If we consider one general case of the transient one-dimensional natural gas flow through pipelines along the pipeline axis while incorporating distributed parameters and time-varying state variables, assuming the cross sectional areas in a pipeline do not change at all or change slowly along the pipeline and the radius of curvature of the pipeline is large enough compared with the diameter of its cross section, the three PDEs in Eq. (3.1), (3.2) and (3.3) are generated (Liu, 2011). These equations involve the space and time dependent density $\rho(x,t)$, pressure $p(x,t)$, velocity $v(x,t)$ and temperature $T(x,t)$, where d is the diameter of the cross-sectional area of a gas duct, t the time in scheduling period, x length scale of the pipeline, g gravitational acceleration, α the elevation angle of the gas pipelines, f the friction factor of gas pipeline, z the height of gas pipeline, e_{in} the specific internal energy of gas, Ω the heat added to the gas and W the work done on the gas by the environment per unit time and unit mass of gas.
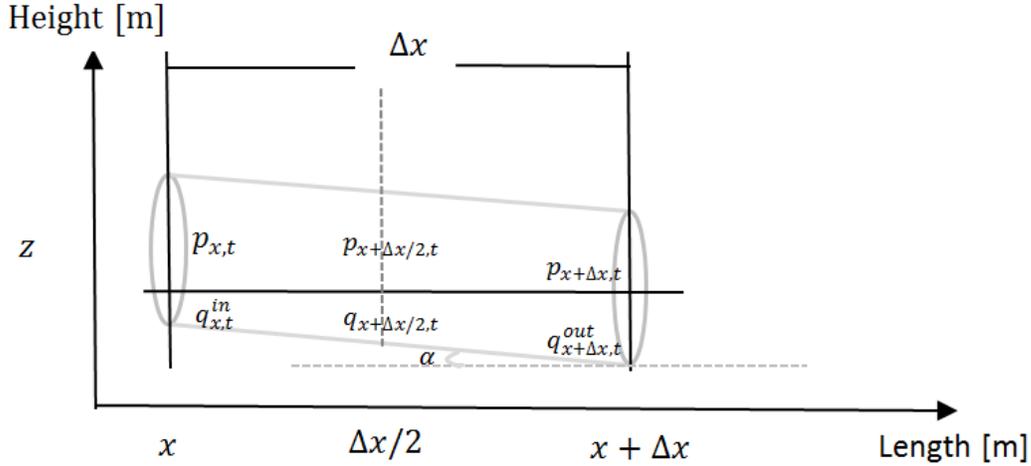
Figure 6 Natural gas pipelines grid

$$\frac{\partial \rho}{\partial t} + \frac{\partial (\rho v)}{\partial x} = 0 \tag{3.1}$$

$$\frac{\partial}{\partial t}\left[\rho \cdot \left(e_{in} + \frac{v^2}{2} + gz\right)\right] + \frac{\partial}{\partial x}\left[\rho \cdot v \cdot \left(e_{in} + \frac{p}{\rho} + \frac{v^2}{2} + gz\right)\right] - \rho \cdot \Omega - \rho \cdot W = 0 \tag{3.2}$$

$$\frac{\partial (\rho v)}{\partial t} + \frac{\partial (\rho v^2)}{\partial x} + \frac{\partial p}{\partial x} + \frac{f \rho v |v|}{2d} + \rho g \sin(\alpha) = 0 \tag{3.3}$$

Eq. (3.1) explains the mass conservation for the one dimensional flow in one pipeline, where the net mass flow rate into (out of) any differential volume of gas in the pipeline is identical with the rate of increase (decrease) of mass within this differential volume.

Eq. (3.2) declares the energy conservation for one dimensional flow in a pipeline, where the total energy change of a system is the same as the addition of the exchange of heat from the external environment and the work done by external forces.

Eq. (3.3) states the momentum equation for one dimensional flow in a pipeline which establishes a connection between the rate of momentum change of the differential volume of gas and the algebraic sum of the forces acting on this volume: pressure force, shear force (due to friction), and net body force (gravitational forces).

Since there are four variables of $\rho(x,t)$, $p(x,t)$, $v(x,t)$ and $T(x,t)$, and three equations in

the PDEs above, another equation of the gas state equation is shown as well, where $R_{specific}$ is

the specific gas constant and Z is the compressibility of the gas.

$$p(x,t) = \rho(x,t) \cdot Z \cdot R_{specific} \cdot T(x,t) \qquad (3.4)$$

Eq. (3.1)–(3.4) can be solved to find the closed form of the gas flows in pipelines, and normally

two conditions are assumed. The first condition is isothermal flow where the temperature is

constant. The gas flows through pipelines are slow enough that heat transfer between gas and

environment is fast resulting in the temperature of gas in a gas duct remaining the same as that of

the outside environment. The other case is adiabatic, in which the heat transfer q equals to zero

and the gas flows are so fast that there is not enough heat transfer happening. In the real case,

neither isothermal nor adiabatic condition happens and there is no thermal equilibrium between

gas duct and the environment, as a consequence of which more mathematical equations will be

required to model the heat conduction process.

Steady state modeling

Steady state flow is one in which those velocity, pressure and cross-sectional areas may

differ from point to point but do not change with time. Hence all those variables we have are

only dependent on the locations. Real operating conditions of gas pipelines allow the adoption of

some simplifying hypotheses in the momentum equation to formulate a tractable optimization

model for large transportation grids. The assumption of isothermal flow is valid due to the slow

transients. Eq. (3.2) is valid because the energy conservation can always be reached by having

heat transfer from the environment (Liu et al., 2011). Then Eq. (3.2) is redundant if we are not

concerned about the exact heat transfer value. The term of $\rho g \sin(\alpha)$ representing the force of

gravity influenced by the slope angle of the pipe is omitted by assuming horizontal pipes.

Additionally those two terms, $\frac{\partial(\rho \cdot v)}{\partial t}$ and $\frac{\partial(\rho \cdot v^2)}{\partial x}$, describing the inertia and kinetic energy

respectively, could be neglected since they contribute less than 1% to the solution of the equation

under normal conditions (Dorin and Toma-Leonida, 2008). Under these assumptions the pressure

gradient and the friction force in Eq. (3.3) could be neglected and Eq. (3.3) is simplified to Eq.

(3.5).

$$\frac{\partial p}{\partial x} + \frac{f \rho v |v|}{2d} = 0 \tag{3.5}$$

Instead of using density and velocity, Eq. (3.1), (3.2) and (3.3) can be written in terms of mass

flows $q(x,t)$ and pressures $p(x,t)$ that are the variables measured in reality. This transformation

is carried out by using the thermodynamic state equation of Eq. (3.4) relating pressure and

density and expressing the mass flow rate at standard conditions as a function of the flow

velocity. Let ρ_0 be the density of gas under standard conditions of 760 millimeters of mercury

barometer and 273.15 degrees Kelvin.

$$q = \frac{\pi d^2}{4} \frac{\rho v}{\rho_0} \tag{3.6}$$

By substituting Eq. (3.4) and (3.6) reduce Eq. (3.1), (3.2) and (3.3) to Eq. (3.7) and (3.8)

(Correa-Posada and Sánchez-Martín, 2014b).

$$\frac{\partial q}{\partial x} + \frac{\pi}{4} \frac{d^2}{R_{specific} TZ\rho_0} \frac{\partial p}{\partial t} = 0 \tag{3.7}$$

$$p \frac{\partial p}{\partial x} + \left(\frac{4}{\pi}\right)^2 \frac{f R_{specific} TZ\rho_0^2}{2d^5} q|q| = 0 \tag{3.8}$$

Given steady state flow condition, all variables are only impacted by the locations. In other

words, $\frac{\partial p}{\partial t}$ equals zero. Thus Eq. (3.7) illustrates that the mass flow rate at any location is the

same and Eq. (3.7) is omitted. Eq. (3.8) is the only required equation to find the closed form of mass flow by using integration. The solution expression is usually called the Weymouth or Panhandle equation. The average flow squared is written as $q|q|$ to note that the model allows bidirectional flows.

$$q_{x+\Delta x/2}\left|q_{x+\Delta x/2}\right| = \left(\frac{\pi}{4}\right)^2 \frac{d^5}{\Delta x f R_{specific} T Z \rho_0^2}\left(p_{x+\Delta x,t}^2 - p_{x,t}^2\right) \tag{3.9}$$

Define $C_{x+\Delta x}$ to be a parameter for pipelines in Eq. (3.10):

$$C_{x,x+\Delta x} = \left(\frac{\pi}{4}\right)^2 \frac{d^5}{\Delta x f R_{specific} T Z \rho_0^2} \tag{3.10}$$

Then Eq. (3.9) could be reduced to Eq. (3.11).

$$q_{x+\Delta x/2}\left|q_{x+\Delta x/2}\right| = C_{x,x+\Delta x}\left(p_{x+\Delta x,t}^2 - p_{x,t}^2\right) \tag{3.11}$$

3.2.2 Active pipelines modeling

Energy and pressure will decrease due to the friction between gas and inner side of pipes and heat transfer between gas and environment. Usually compressor stations are installed at 50–100 mile intervals along the pipelines to compensate for the pressure loss in the transmission processes which consume 3% to 5% of the total gas transported (Wu et al., 2000). The natural gas flows through the compressor stations depend on the pressure ratio, working power and some other parameters of a compressor station and thus could be modeled as with the assumption of steady state flow:

$$q_{x+\Delta x/2} = \text{sgn}(p_{x+\Delta x,t} - p_{x,t})\frac{h_{cp,t}}{K_{2,cp} - K_{1,cp}\left[\frac{\max(p_{x+Dx,t}, \ p_{x,t})}{\min(p_{x+Dx,t}, \ p_{x,t})}\right]^a} \tag{3.12}$$

$$H_{cp}^{min} \le h_{cp,t} \le H_{cp}^{max} \tag{3.13}$$

$$R^{min} \leq \frac{\max(p_{x+\Delta x,t},\ p_{x,t})}{\min(p_{x+\Delta x,t},\ p_{x,t})} \leq R^{max} \qquad (3.14)$$

where cp is the index of compressor stations and $\alpha, K_{1,cp}, K_{2,cp}$ are empirical parameters of the

compressor design. $H_{cp}^{min}, H_{cp}^{max}, R^{min}, R^{max}$ are the minimum or maximum compressors'

working power and minimum or maximum pressure ratio of a compressor station respectively.

$h_{cp,t}$ is the working power of compressor, and the amount of gas the compressor station

consumes is governed by:

$$q_{cp,t} = C_{cp} + B_{cp} \times h_{cp,t} + A_{cp} \times h_{cp,t}^2 \qquad (3.15)$$

where C_{cp}, B_{cp}, A_{cp} are parameters of gas consuming function of compressor cp. The decision

variables of compressor system would be $h_{cp,t}, p_{x+\Delta x,t}$ and $p_{x,t}$.

However, the model above is quite complicated and nonlinear. We could also introduce two

new variables, $pr_{j,ajp,t}^{left}$ and $pr_{j,ajp,t}^{right}$, to describe the pressure at two sides of the compressors. So

we can model the active pipelines in simplified way which is similar to the passive pipeline by

ignoring the energy consumption of compressors and apply the Weymouth equation to model gas

flow in pipelines.

3.3 Natural Gas Storage Modeling

As mentioned above, natural gas storage capacity is always divided into cushion capacity and

working capacity. In other words, we have $level_{stor,t} = cuslevel_{stor,t} + worklevel_{stor,t}$. The injection

and extraction rates of the storage facilities vary with their current storage level. Figure 7

illustrates the intuitive concept of higher working capacity resulting in higher extraction rate and

lower injection rate. Nico asserts that the maximum injection rate is a strictly decreasing convex

function of the storage level. On the basis of Bernoulli's principle in Eq. (3.16), where in fluid

dynamics for an inviscid flow of a non-conducting fluid, an increase in the speed of the fluid

occurs simultaneously with a decrease in pressure or a decrease in the fluid's potential energy

(Nico 2012).

$$\frac{v^2}{2} + gz + \frac{p}{r} = constant \tag{3.16}$$

Thompson and Nico derived the relations between storage-flow limits to the current level of

stored gas to link the effective storage-flow limits to the current level of stored gas. Moreover,

they computed $K_{stor}^{WD}, K_{stor}^{INJ\_1}, K_{stor}^{INJ\_2}$, which are proportionality factors that represent the

characteristics of the storage when the flow rates are mutually exclusive (Thompson et al, 2009;

Nico, 2012).

$$q_{stor,t}^{WD} \leq K_{stor}^{WD} \sqrt{worklevel_{stor,t}} \tag{3.17}$$

$$q_{stor,t}^{INJ} \leq K_{stor}^{INJ\_1} \sqrt{\frac{1}{cuslevel_{stor,t} + worklevel_{stor,t}} + K_{stor}^{INJ\_2}} \tag{3.18}$$
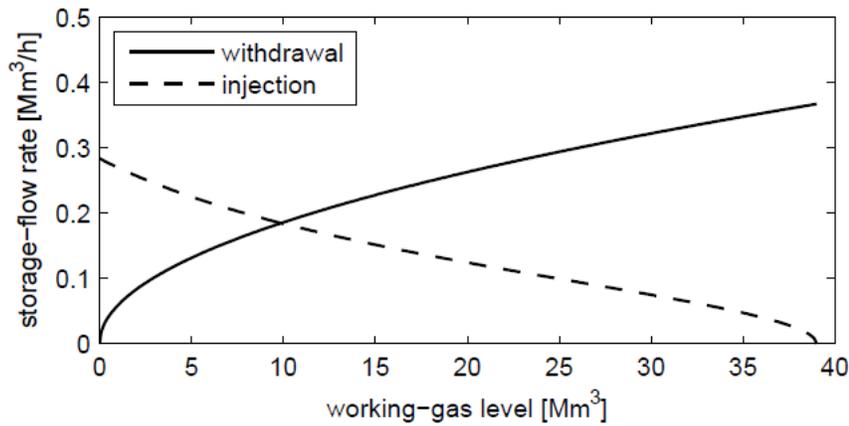
Figure 7 Withdrawal and injection limits according to the level of working gas in storage (Nico, 2012)

With the object of solving the total system efficiently, an assumption of constant hourly flow rate

into or out of the storage facilities is applied in the combined system.

CHAPTER 4. ELECTRIC POWER SYSTEM WITH WIND ENERGY

4.1 Introduction to the Electric Power System

An electric power system is a network of electrical components constitutive of consumption, generation, transmission and distribution. The independent system operator (ISO) is set up to operate the electric power system and facilitate a competitive market for the power generation and retail process. The ISO with powerful computational tools, involving market monitoring, ancillary services auctions and congestion management, is independent of other individual market participants of generators, transmission owners, distribution companies and end customers. The Federal Energy Regulatory Commission (FERC) Order No. 888 established unbundled electricity markets in the restructured electricity industry. Energy and ancillary services were offered as unbundled services, and generation companies (GENCOs) competed for selling energy to customers by submitting competitive bids to the electricity markets, where they maximized their profits regardless of the system-wide profit. And the ISO would run this equilibrium model about electric power supply from GENCOs and demand from distribution centers to get the best system-wide working schedule with which each individual participant in the system is required to comply.

4.1.1 Consumption

Electric power consumption is an important indicator of each country's economic, industrial and social development. Electricity consumption per person and electrification level of one country indicates its wellness and living standard. The electricity consumption is classified into areas including residential, commercial, industrial, transportation and others. Residential and

commercial customers expended most electric power in the last ten years, taking account of

almost 37% and 35% of the total electricity consumption separately. Industrial customers

consume nearly 27% of the total electricity consumption, and transportation takes account of the

remaining 0.2% percent of the whole electricity consumption. Each area takes an approximately

stable percent of the total consumption. The order of the retail price for each from high to low

would be residential, transportation, commercial and industrial. The price of electricity will

increase with the annual rate of 2.7%, 2.2%, 3.2% and 3.9% separately for residential,

transportation, commercial and industrial areas, according to the projection of EIA. Total energy

purchased in 2015, including electric power producers and on-site power generations, reached

3,836 billion kilo-watthours (KWh) and is projected to increase 0.8% annually to reach 4,797

billion KWh in 2040 (EIA 2015a).

4.1.2 Generation

The principal fuels of electric power generation are coal, nuclear, renewables, natural gas,

petroleum and other liquids. The nuclear and coal's percentage will decrease by 7% and 5%,

respectively, due to the stability of electric power generation from these two fuels and the

expansion of total generation. In the longer period, natural gas will fuel more than 60% of the

new electric power generation from 2025 to 2040, and renewable energy will supply most of the

remainder. Figure 8 shows the trend of fuel type distributions in the whole and renewable

electricity generation from 2000 to 2040, during which the generation proportions of hydropower

and municipal solid waste and landfill gas (MSW/LFG) are almost stable and the ratio of

remaining fuel types increase dramatically. One reason for this change of electric fuel structure is

that gas price has stayed low and stable since 2009 thanks to the exploitation of shale gas. The

research and technology improvement in shale gas exploitation and combined cycle natural gas plants (CCGP) is another reason for the structural change of electric fuels. The International Energy Administration reports that combined cycle gas plants have a higher average efficiency, ranging from 52-60%, than supercritical coal plants and ultra-supercritical coal plants whose average efficiency is 46% and 50% respectively. Moreover, natural gas fueled power generators have a shorter construction period of about 36 months than coal plants whose construction period is about 72 months. Beyond that, combined cycle power plants are able to start in 30 minutes and combustion engine power plants can be started up and achieve full load in less than 10 minutes, while the coal or nuclear power plants require several hours to start (Macmillan et al., 2013).
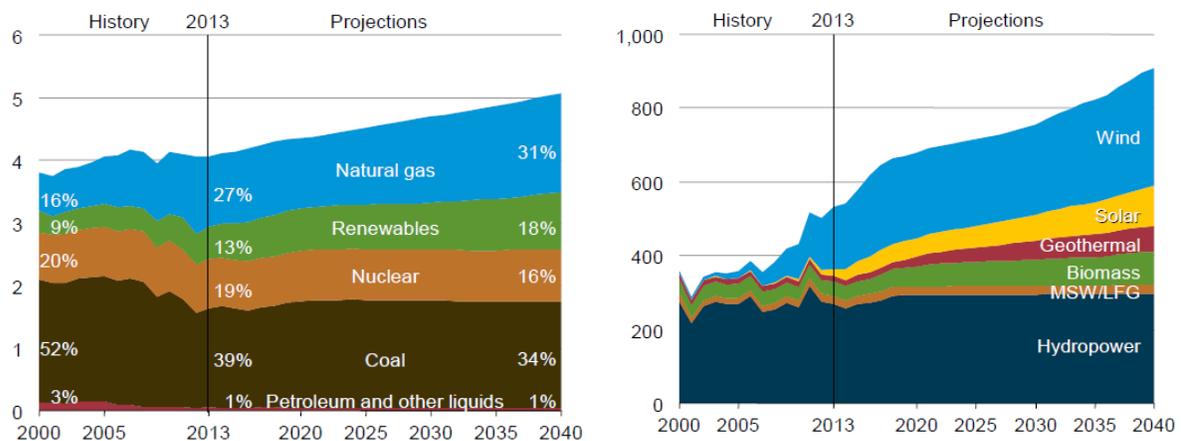
Figure 8 Electricity generation and renewable electricity generation by fuel in the reference case, 2000-2040 (KWh) (EIA, 2015a)

4.1.3 Transmission and distribution

After electricity is produced, an intricate transmission and distribution network is requisite to transmit the generated electricity to ultimate users. To obtain high transmission efficiency and reduce cable sizes and voltage drops in power lines, transformers are essential to raise electricity voltage up to 400,000 volts for long distance travels. High voltage transmission lines carry

electricity long distances to a substation which is near businesses, factories and homes and where transformers reduce the very high voltage electricity back to low voltage electricity for usage. In these substations, a dynamic equilibrium of electric demand and supply is guaranteed and corresponding power dispatch schedule is built to keep the electric power system functioning stably. Then the distribution network's job is to transmit the lower voltage electricity to the scheduled areas. How to combine the unstable electricity generation from renewable fuels like wind into the regular electric power transmission and distribution network is one of the most crucial issues when discussing power transmission and distribution system. The other topic absorbing attention is how to enhance the transmission capacity due to the increasing electric power demand and disparities in locational generation prices and capacities.

4.2 Electric Power Generation Model

For generation companies (GENCOs), generating cost comes from four portions including start-up, shut- down, no-load and incremental energy costs, where the first two are the cost of bringing an off line generation resource online or in reverse. As shown in Figure 9, once a generator is started up, only when the production level of this generator is more than the synchronized level the excess portion is able to be injected into the grid. Consequently, no-load cost representing the fees required by the GENCO for operating a generating unit in a state of and synchronized and injecting 0 MW into the grid is applied to characterize the cost of keeping a generator in synchronized state and incremental energy cost is proposed to describe the cost of certain amount of production output. Then for each hour t the generating cost for each GENCO would be:

$$GC(t) = StartupCost(t) + ShutdownCost(t) + NoLoadCost(t) + IncEnergyCost(p_t) \qquad (4.1)$$

where $StartupCost(t^*)$ and $ShutdownCost(t^*)$ represents start-up and shut-down costs at time

t^* respectively, $NoloadCost(t)$ the cost claimed by the GENCO to operate a generating unit in

the synchronized state, and $IncEnergyCost(p_t)$ the variable cost for generating certain watts of

output p_t. As shown in Figure 9, several minutes are needed to start up a generator to its

synchronized state. Although for various generators there are different start-up or shut-down

hours, the natural gas fueled electric power generator is one of the fastest-response generators

with the minimum number of start-up or shut-down hours. In order to simplify the calculation

process of start-up and shut-down costs, we assume the start-up and shut-down costs are incurred

in one hour and the incremental cost of energy is constant. Then the total generating cost is:

$$GC(t) = C_{ug}^{SU}\, su_{ug,t} + C_{ug}^{SD}\, sd_{ug,t} + C_{ug}^{NL} u_{ug,t} + C_{ug}^{INC}\, gpp_{ug,t} \qquad (4.2)$$

in which $su_{ug,t}$, $sd_{ug,t}$, $u_{ug,t}$ are binary variables to describe if generator ug at time t is started

up, shut down, on line or not respectively, and $gpp_{ug,t}$ is the production output. The parameters,

C_{ug}^{SU} ($\$/h$), C_{ug}^{SD} ($\$/h$), C_{ug}^{NL} ($\$/h$) and C_{ug}^{INC} ($\$/MWh$), represent start-up cost, shut-down cost,

no-load cost and incremental energy cost respectively.
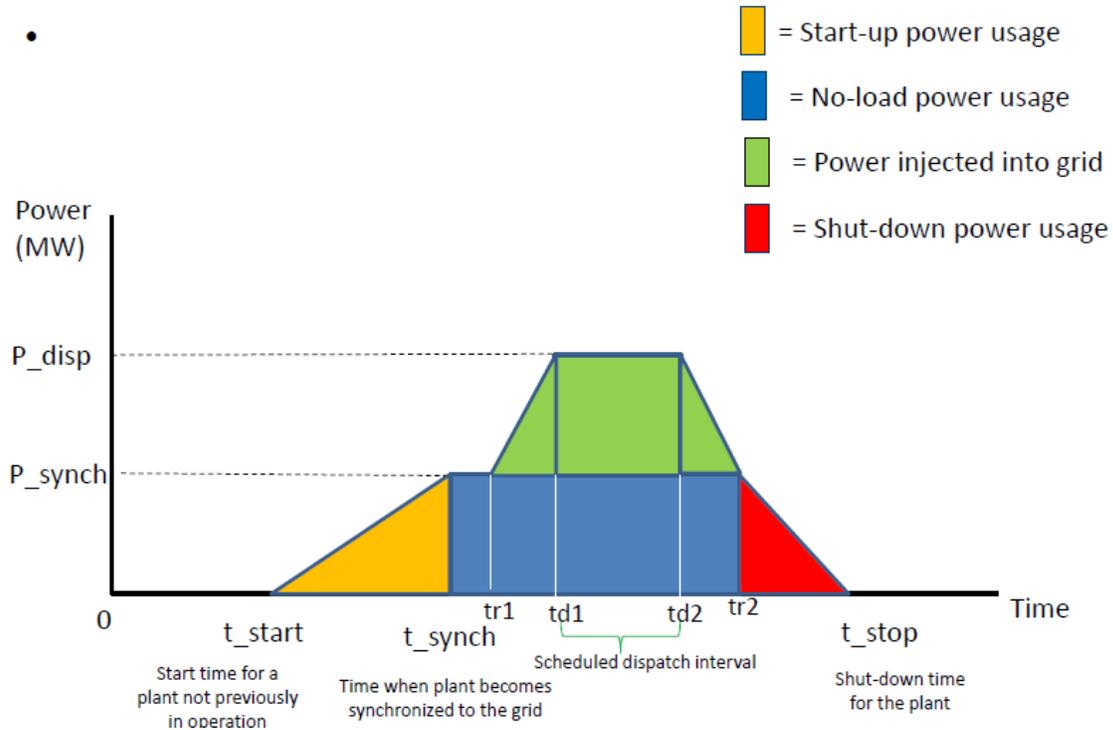
Figure 9 Power plant cost (Chen, 2014)

On the generation constraints aspect, for each node, an equilibrium state of the total electric power demand, the total electric power supply from the gas and wind, power inflow and outflow and the non-served power amount exists at any time. Those gas fueled power generators come with constraints of their operational status, ramp up and down rate and minimum on and off time. The operational status constraints state the relationship between the generators' operational status such as one generator cannot be started up or shut down simultaneously. Moreover, an upper bound and lower bound exist for the ramp up and down rates and the production level. In addition, once a generator is started up (shut down), it is requisite to maintain the on (off) status for a certain number of hours.

4.3 Electric Power Transmission Model

With the DC power flow approximation, ignoring the resistance and reactive power, the

power flow could be described as in Eq. (4.4) given all voltage magnitudes being 1 p.u. and all

voltage angles being small. Variable $\theta_{i,t}$ is the voltage angle for power node for each hour, and

variable $pf_{i,ip,t}$ is the amount of power flow from power node i to ip for each hour. Parameters

$X_{i,ip}$ and $\overline{PF_{i,ip}}$ are the reactance and the maximum power flow, respectively, of the transmission

line from node i to ip. And a negative flow from node i to ip represents the flow direction is

from ip to i.

$$-\overline{PF_{i,ip}} \leq pf_{i,ip,t} \leq \overline{PF_{i,ip}} \tag{4.3}$$

$$pf_{i,ip,t} = \frac{\theta_{i,t} - \theta_{ip,t}}{X_{i,ip}} \quad for \ \forall ip \in c_I(i), \ for \ \forall i \in I \tag{4.4}$$

The first constraint (4.3) enforces the upper and lower bound of transmission capacity and the

second constraint is calculating the amount of electricity flow between two electric nodes.

Moreover, for each node in the power system, a dynamic electric power balance of power inflow

and outflow is required.

CHAPTER 5. COMBINED MODEL OF NATURAL GAS AND ELECTRIC POWER SYSTEM WITH WIND ENERGY

5.1 Notations

Both the natural gas system and the power system are analogized as a network problem which is composed of several nodes and lines (figure 10). We call the nodes in the natural gas system gas nodes, while those nodes in the power system are named power nodes. The gas nodes (circles in Figure 10) include gas supply nodes, transmission and distribution nodes and gas demand nodes. The power nodes (bars in Figure 10) consist of power plants, power transmission nodes and power demand nodes. Lines in the gas system and the power system represent pipelines and transmission lines, respectively. The dashed lines illustrate that some of the gas demand nodes supply the gas demands of gas fueled power generators. The notations for sets, indexes, parameters and decision variables are listed below:
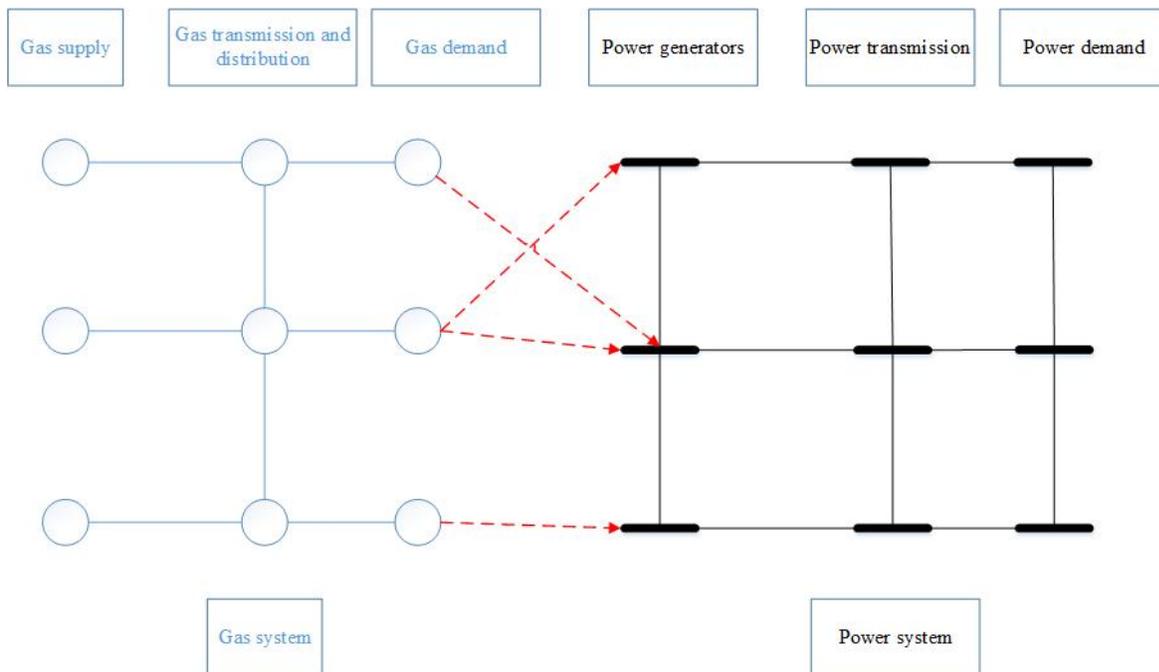
Figure 10 Network model

5.1.1 Indexes and Sets

$j \in J$	Set of gas nodes.
$w \in W(j)$	Set of gas wells in gas node j.
$jp \in c_J(j)$	Set of nodes connected to node j in the gas nodes system.
$pjp \in c_J^P(j)$	Set of gas nodes connected to node j by passive pipelines.
$ajp \in c_J^A(j)$	Set of gas nodes connected to node j by active pipelines.
$cp \in CP(j, ajp)$	Set of gas compressors between node j and ajp, $\forall ajp \in c_J^A(j)$.
$stor \in STOR(j)$	Set of gas storage facilities in gas node j.
$i \in I$	Set of power nodes.
$ip \in c_I(i)$	Set of nodes connected to electricity node i in the power system.
$t \in T$	Hourly periods, running from 1 to 24.
$ug \in UG(i)$	Set of gas-fueled power plants in power node i.
$uw \in UW(i)$	Set of wind power plants in power node i.
$p_{j,jp} \in P_{j,jp}$	Set of segments in the approximation of nonlinear gas system constraints for the pipeline from node j to jp.
$s \in S$	Set of daily wind power supply scenarios.

5.1.2 Parameters

$\overline{GP_w}$	Maximum daily output of gas well w [kcf/day].
$\underline{GP_w}$	Minimum daily output of gas well w [kcf /day].
C_w^G	Cost of natural gas from gas well w [\$/kcf].
$C_{j,jp}$	Pipeline constant that depends on temperature, length, diameter, friction and gas consumption, $jp \in c_J(j)$ [kcf/Psig]
$C_{j,ajp}^{left}$	Pipeline constant that depends on temperature, length, diameter, friction and gas consumption for the pipelines connecting compressor and node j in pipeline from node j to ajp, $\forall ajp \in c_J^A(j)$ [kcf/Psig]

$C_{j,ajp}^{right}$	Pipeline constant that depends on temperature, length, diameter, friction and gas consumption for the pipelines connecting compressor and node ajp in pipeline from node j to ajp, $\forall ajp \in c_J^A(j)$ [kcf/Psig]
$\overline{pr_j}$	Maximum pressure of gas node j [Psig].
$\underline{pr_j}$	Minimum pressure of gas node j [Psig].
$\overline{Cap_{stor}}$	Maximum storage level for storage facility $stor$ [kcf] (cushion gas plus the maximum working gas amount).
$\underline{Cap_{stor}}$	Minimum storage level for storage facility $stor$ [kcf] (cushion gas amount).
$LEVEL_{stor}^{initial}$	Initial gas storage level of $stor$ [kcf].
Q_{stor}	Maximum value for the result of outflow minus inflow of storage $stor$ [kcf/h].
C_{stor}^{STOR}	Cost of the gas from storage $stor$ [\$/kcf].
$GF_{j,jp}^{p_{j,jp}}$	Gas flow of the $p_{j,jp}$th segment when doing approximation of the nonlinear constraints [kcf].
$\tau_{j,ajp}$	Maximum pressure increase ratio for the active pipeline from j to ajp, $ajp \in c_J^A(j)$.
$\Delta\pi_{j,jp}^{p_{j,jp}}$	Pressure-square gap of the $p_{j,jp}$th segment in hour t when doing the approximation of the nonlinear constraints for pipeline from node j to jp.
$GD_{j,t}^{pred}$	Prediction of next day's non-electric gas demand in node j at hour t [kcf/h].
C_j^{NSG}	Penalty for non-served gas for gas node j [\$/kcf].
Bf_{ug}	Intercept of gas consuming function of gas fueled power generator ug [kcf/MWh].
Cf_{ug}	Slope of gas consuming function of gas fueled power generator ug [kcf/h].
C_{ug}^{SD}	Shut-down cost of gas power generator ug [\$].
C_{ug}^{SU}	Start-up cost of gas power generator ug [\$].
C_{ug}^{INC}	Incremental production cost of gas power generator ug [\$/MWh].
C_{ug}^{NL}	No load cost of gas power generator ug [\$/h].
C_i^{NSP}	Penalty for non-served power for electricity node i [\$/MWh].

$\overline{GPP_{ug}}$	Maximum output of gas fueled power generator ug if it is on [MW/h].
$\underline{GPP_{ug}}$	Minimum output of gas fueled power generator ug if it is on [MW/h].
$GPP_{ug}^{initial}$	Initial power production output for gas fueled power generator ug [MW/h].
$X_{i,ip}$	Transmission line reactance, $ip \in c_I(i)$ [p.u.].
$\overline{PF_{i,ip}}$	Maximum power flow from node i to ip, $ip \in c_I(i)$ [MW] .
RU_{ug}	Maximum ramp up rate of gas fueled power generator ug [MW/h].
RD_{ug}	Maximum ramp down rate of gas fueled power generator ug [MW/h].
$SD_{ug}^{initial}$	Initial shut-down status of gas fueled power generator ug, binary.
$SU_{ug}^{initial}$	Initial start-up status of gas fueled power generator ug, binary.
$U_{ug}^{initial}$	Initial on or off status of gas fueled power generator ug, binary. 1 if gas fueled power generator ug is in on status initially and 0 otherwise.
TU_{ug}	Minimum up time of generator ug [hours].
TD_{ug}	Minimum down time of generator ug [hours].
$TU_{ug}^{initial}$	Initial up time of generator ug [hours].
$TD_{ug}^{initial}$	Initial down time of generator ug [hours].
$PD_{i,t}^{pred}$	Prediction of next day's power demand in node i at hour t [MW/h].
$\overline{WPP_{uw,t}}$	Available power from wind power plant uw at hour t [MW].
WR_t	Reserve margin for wind power in hour t, percentage.
$MAXSP_{ug}$	Maximum spinning reserve for generator ug as a percentage of total capacity.
C^{NSR}	Penalty for non-served reserve [\$/MWh].
$Prob^s$	Probability of scenario s.

5.1.3 Binary Decision Variables

$su_{ug,t}$	Start-up: 1 if gas unit ug is started up in time t and 0 otherwise.

$sd_{ug,t}$	Shut-down: 1 if gas unit ug is shut down in time t and 0 otherwise.
$u_{ug,t}$	Commitment: 1 if gas unit ug is on in time t and 0 otherwise.
$y_{j,jp,t}^{p_{j,jp}}$	Indicator: 1 if $p_{j,jp}$ th segment is chosen in hour t in the approximation of nonlinear constraints for pipeline from j to jp and 0 otherwise.

5.1.4 Continuous Decision Variables

gp_w	Daily gas production in well w [kcf].
$gf_{j,jp,t}$	Gas pipeline flow out of node j at time t [kcf], $jp\epsilon c_J(j)$. Positive if the gas flow is from node j to jp and negative otherwise.
$nsg_{j,t}$	The non-served gas amount in node j at hour t [kcf].
$pr_{j,t}$	Gas node pressure in node j at hour t [Psig].
$pr_{j,ajp,t}^{left}$	The pressure of the node of the compressor which is close to node j in active pipeline from node j to node ajp, $ajp \in c_J^A(j)$ [Psig].
$pr_{j,ajp,t}^{right}$	The pressure of the node of the compressor which is close to node ajp in active pipeline from node j to node ajp, $ajp \in c_J^A(j)$ [Psig].
$\pi_{j,t}$	Square of pressure at gas node j at hour t [Psig^2].
$\Delta\pi_{j,jp,t}$	Pressure square difference in pipeline of node j and node jp at hour t [Psig^2]
$\delta_{j,jp,t}^{p_{j,jp}}$	Linear combination coefficients for function of the gas flow of the $p_{j,jp}$ th segment when doing the approximation of the nonlinear constraints for pipeline from node j to jp in hour t.
$level_{stor,t}$	Storage level of storage facility $stor$ at the end of hour t [kcf].
$q_{stor,t}^{OUT}$	Outflow of storage $stor$ at hour t [kcf/h].
$q_{stor,t}^{IN}$	Inflow of storage $stor$ at hour t [kcf/h].
$\theta_{i,t}$	Voltage angles for power node i at hour t [rad].
$gpp_{ug,t}$	Power production above $\underline{P_{ug}^P}$ from gas fueled power generator ug in hour t [MW].
$pf_{i,ip,t}$	Power flow out of node i at time t [MW], $ip\epsilon c_I(i)$. Positive if the gas flow is from node i to ip and negative otherwise.

$egd_{ug,t}$	Gas demand of gas power generator ug at hour t [kcf/h].
$nsp_{i,t}$	The non-served power amount in node i at hour t [MWh].
$wpp_{uw,t}$	Power production from wind power plant uw in hour t [MW].
$r_{ug,t}$	Operating reserve provided by generator ug in hour t [MW].
nsr_t	The unsatisfied reserve amount at hour t [MW].

5.2 Natural Gas System Model

5.2.1 Natural gas model assumptions

The costs of the natural gas system include penalties for non-served natural gas, supply cost of gas wells and the net cost of gas flow from the storage facilities, ignoring the cost of compressor stations and other corresponding cost of natural gas system.

The constraints include the dynamic equilibrium of natural gas demand and supply for each node at each hour in view of non-served gas and natural gas flow in pipelines and from storage facilities. In addition, upper and lower bounds are essential for the natural gas pressure at each node, as well as flow rates and storage levels of each storage facility. Although the upper bound of extraction and injection rate of natural gas in storage facilities strongly depends on the storage level, in order to simplify the model and solve a tractable linear problem, we assume a constant hourly injection and extraction rate of natural gas in the storage facilities. This rate is used in the constraints for storage level, injection and extraction rates in storage facilities for consecutive periods. Last but certainly not least, with regard to the active pipelines with compressor stations, the compressor factor is proposed to represent the maximum pressure enhancement ratio. Supposing a steady state flow, the Weymouth equation is applied to the gas flow in pipelines, while for passive pipelines or active pipelines with compressors not working the flow direction is

from the node with a higher pressure to the node with a lower pressure and for active pipelines with compressors working the flow direction will be reversed. A nonlinear and non-convex optimization model is formulated to model the natural gas system owing to the Weymouth equation being nonlinear and non-convex. And correspondingly the incremental method is applied to the Weymouth equation to approximate the nonlinear constraints with linear ones, as a result of which a mixed linear integer natural gas system model is formulated.

5.2.2 Nonlinear natural gas system model

The formulation of the natural gas system optimization is as follows:

- *Objective function*: Minimize the total cost of the natural gas system including the penalties of non-served gas, supply cost of gas wells and the net cost of gas flow from the storage, ignoring the compressor stations' cost and other costs.

$$\min\left\{\sum_{t=1}^{24}\left[\sum_{j\in J}C_j^{NSG}nsg_{j,t}+\sum_{stor\in STOR}C_{stor}^{STOR}q_{stor,t}^{OUT}\right]+\sum_{w\in W}C_w^G gp_w\right\} \tag{5.1}$$

- *Gas flow equilibrium constraints*: At each hour for each node in the natural gas network, the total natural gas flow out of this node including gas outflow through pipelines, non-electric and electric gas demand equals the non-served natural gas amount plus the total natural gas inflow including inflow through pipelines and net supply from the storage facilities and wells.

$$nsg_{j,t}+\sum_{w\in W(j)}\frac{gp_w}{24}+\sum_{stor\in STOR(j)}(q_{stor,t}^{OUT}-q_{stor,t}^{IN})\geq\sum_{jp\in c_J(j)}gf_{j,jp,t}+GD_{j,t}^{pred}+\sum_{ug\in UG(j)}egd_{ug,t} \tag{5.2}$$

$$\forall j\in J, t\in T$$

- *Gas storage flow constraints*: Eq. (5.3) and (5.4) state that upper and lower bounds exist for the storage level and flow rate of each storage facility. Eq. (5.5) illustrates that storage

levels of consecutive hours are connected by the storage flow rate, and Eq. (5.6) is the corresponding boundary condition. Eq. (5.7) declares that the flow rate will be bounded such that the storage level of storage facilities will always be bounded between $\underline{Cap_{stor}}$ and $\overline{Cap_{stor}}$.

$$\underline{Cap_{stor}} \leq level_{stor,t} \leq \overline{Cap_{stor}} \qquad \forall stor \in STOR, \forall t \in T \tag{5.3}$$

$$-Q_{stor} \leq (q_{stor,t}^{OUT} - q_{stor,t}^{IN}) \leq Q_{stor} \quad \forall stor \in STOR, \forall t \in T \tag{5.4}$$

$$level_{stor,t} = level_{stor,t-1} - q_{stor,t}^{OUT} + q_{stor,t}^{IN} \qquad \forall stor \in STOR, \forall t \in \{2,3,...,24\} \tag{5.5}$$

$$level_{stor,1} = LEVEL_{stor}^{initial} - q_{stor,1}^{OUT} + q_{stor,1}^{IN} \quad \forall stor \in STOR, \forall t \in T \tag{5.6}$$

$$level_{stor,t-1} - \overline{Cap_{stor}} \leq q_{stor,t}^{OUT} - q_{stor,t}^{IN} \leq level_{stor,t-1} - \underline{Cap_{stor}}$$
$$\forall stor \in STOR, \forall t \in \{2,3,...,24\} \tag{5.7}$$

- *Maximum and minimum pressure*: Each node has upper and lower bounds for the natural gas pressure.

$$\underline{pr_j} \leq pr_{j,t} \leq \overline{pr_j} \qquad \forall j \in J, \forall t \in T \tag{5.8}$$

- *Gas flow in pipeline:* The Weymouth equation is applied to characterize gas flows in passive pipelines.

$$gf_{j,pjp,t} = \text{sgn}(pr_{j,t} - pr_{pjp,t})C_{j,pjp}\sqrt{|\left(pr_{pjp,t}\right)^2 - \left(pr_{j,t}\right)^2|} \mid \forall pjp \in c_J^P(j), \forall t \in T \tag{5.9}$$

$$\text{sgn}(pr_{j,t} - pr_{pjp,t}) = \begin{cases} 1 & pr_{j,t} > pr_{pjp,t} \\ 0 & pr_{j,t} = pr_{pjp,t} \quad \forall j, \in J, \forall pjp \in c_J^P(j), \forall t \in T \\ -1 & pr_{j,t} < pr_{pjp,t} \end{cases} \tag{5.10}$$

- *Active pipeline constraints:* There is an upper bound of the pressure increase ratio in active pipelines and the Weymouth equation is applied to find the gas flows in pipelines. A decision variable $pr_{j,ajp,t}^{left}$ is introduced to represent the pressure of the side of the compressor which is close to gas node j. Similarly, $pr_{j,ajp,t}^{right}$ is the pressure of the side of

the compressor close to node jp. A simplified model of compressors is proposed in which the outlet pressure increased as a function of the inlet pressure, regardless of flow.

➢ If we consider the compressor is working and the flow is from node j to jp, then the objective of compressor is to increase the pressure of gas flow through it. In other words, $pr^{right}_{j,ajp,t} \geq pr^{left}_{j,ajp,t}$. In addition, because of the working power limit of compressor stations, $pr^{left}_{j,ajp,t} \leq pr^{right}_{j,ajp,t} \leq pr^{left}_{j,ajp,t}\tau_{j,ajp}$ or $\dfrac{pr^{right}_{j,jp,t}}{\tau_{j,ajp}} \leq pr^{left}_{j,ajp,t} \leq pr^{right}_{j,ajp,t}$.

➢ If the flow direction is reversed and the compressor is still working, then

$$pr^{right}_{j,ajp,t} \leq pr^{left}_{j,ajp,t} \leq pr^{right}_{j,ajp,t}\tau_{j,ajp} \text{ or } \dfrac{pr^{left}_{j,jp,t}}{\tau_{j,ajp}} \leq pr^{right}_{j,ajp,t} \leq pr^{left}_{j,ajp,t}.$$

➢ If the compressor is not working, then $pr^{right}_{j,ajp,t} = pr^{left}_{j,ajp,t}$.

Hence the relationship of the pressure of two end nodes of compressor stations could be described as Eq. (5.11). Either the pressure gap between node j and left hand side or the pressure gap between the right hand side node and node jp could be utilized to find the mass flow amount by using Weymouth equation in Eq. (5.12) and (5.13).
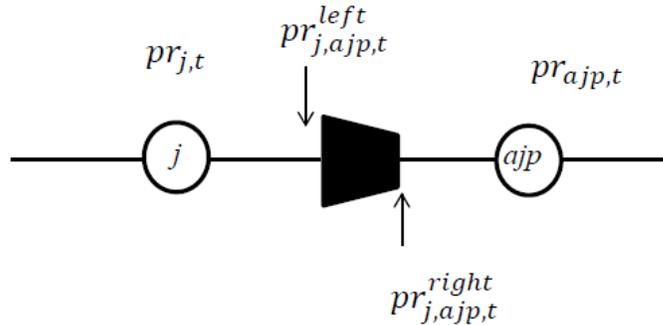
Figure 11 Active pipeline

$$\frac{pr_{j,jp,t}^{right}}{\tau_{j,ajp}} \le pr_{j,ajp,t}^{left} \le pr_{j,ajp,t}^{right}\tau_{j,ajp} \quad ajp \in c_J^A(j) \tag{5.11}$$

$$gf_{j,ajp,t} = \text{sgn}(pr_{j,ajp,t}^{right} - pr_{ajp,t})C_{j,ajp}^{right}\sqrt{\left|\left(pr_{p,ajp,t}^{right}\right)^2 - \left(pr_{jp,t}\right)^2\right|} \quad \forall pr_{jp,t} \in c_J^{AP}(j) \tag{5.12}$$

$$gf_{j,ajp,t} = \text{sgn}(pr_{j,t} - pr_{j,ajp,t}^{left})C_{j,ajp,t}^{left}\sqrt{\left|\left(pr_{p,ajp,t}^{left}\right)^2 - \left(pr_{j,t}\right)^2\right|} \quad \forall pr_{p,ajp,t}^{left} \in c_J^{AP}(j) \tag{5.13}$$

5.2.3 Mixed integer linear natural gas system model
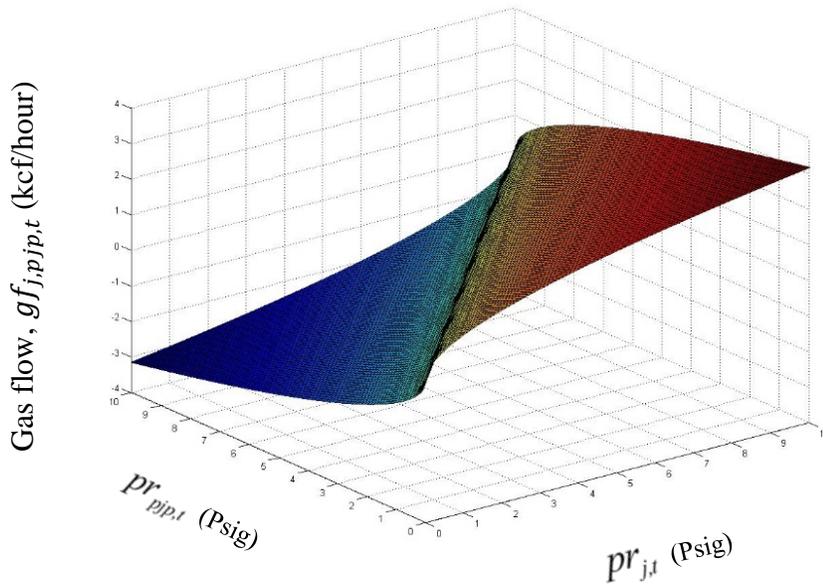
Figure 12 Gas flows in pipelines by applying Eq. (5.9) and (5.10) ($C_{j,pjp}$=1)

According to the Weymouth equation, the gas flow in a passive pipeline is a continuous,

nonlinear and non-convex function of the pressures of these two end nodes of the pipeline as

illustrated in Figure 12. Accordingly, an incremental method is applied to approximate the

nonlinear constraints by using linear constraints and a corresponding MILP natural gas model is

formulated. As illustrated in Figure 13, Markowitz and Manne (1975) formulates a continuous

variable δ_p and a binary variable of y_p for each segment, where δ_p represents the portion of each

segment and binary variable y_p forces that if an interval is chosen then all intervals to its left

must be completely used. And then the nonlinear relation for one dimension problem can be

approximated as:

$$h(x) \approx h(x_1) + \sum_{p \in P} \left[h(x_{p+1}) - h(x_p) \right] \delta_p \qquad (5.15)$$

$$x = x_1 + \sum_{p \in P} (x_{p+1} - x_p) \delta_p, \qquad (5.16)$$

$$\delta_{p+1} \leq y_p \leq \delta_p, \forall p \in P - 1 \qquad (5.17)$$

$$0 \leq \delta_p \leq 1, y_p \text{ binary}, \forall p \in P \qquad (5.18)$$

where the last two constraints are identical with the following constraint:

$$\text{if } \delta_p > 0 \text{ with } 2 \leq p \leq P - 1, \text{ then } \delta_{pp} = 1 \ \forall 1 \leq pp < p.$$
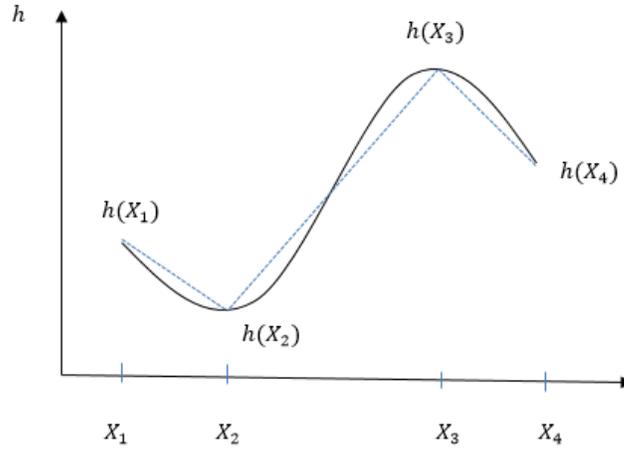
Figure 13 Incremental approximation of a nonlinear separable function

Square of pressures and pressure square gap are defined in Eq. (5.19) and (5.20) respectively.

Then we can rewrite the Weymouth equation in Eq. (5.21).

$$\pi_{j,t} = \left(pr_{j,t} \right)^2 \quad \forall j, t \qquad (5.19)$$

$$\Delta \pi_{j,jp,t} = \pi_{j,t} - \pi_{jp,t} \quad \forall jp \in c_J(j) \qquad (5.20)$$

$$gf_{j,pjp,t} = \text{sgn}(\Delta \pi_{j,pjp,t}) C_{j,pjp} \sqrt{|\Delta \pi_{j,pjp,t}|} \ \forall pjp \in c_J^P(j), \forall t \in T \qquad (5.21)$$

Thus, the Weymouth equation has only one variable and can be linearized by applying the

incremental method to the Weymouth equation with $x = \Delta\pi_{j,jp,t}$, $h(x) = \text{sgn}(x)C_{j,pjp}\sqrt{|x|}$. The

linearization process is done by applying Eq. (5.22)-(5.26).

$$\Delta\pi_{j,jp,t} = \Delta\pi_{j,jp,t}^1 + \sum_{p_{j,jp}\in P}(\Delta\pi_{j,jp,t}^{p_{j,jp}+1} - \Delta\pi_{j,jp,t}^{p_{j,jp}})\delta_{j,jp,t}^{p_{j,jp}} \tag{5.22}$$

$$gf_{j,jp,t} = GF_{j,jp,t}^1 + \sum_{p_{j,jp}\in P}(GF_{j,jp,t}^{p_{j,jp}+1} - GF_{j,jp,t}^{p_{j,jp}})\delta_{j,jp}^{p_{j,jp}} \tag{5.23}$$

$$GF_{j,jp,t}^{p_{j,jp}} = sgn(\Delta\pi_{j,jp,,t}^{p_{j,jp}})C_{j,jp}\sqrt{|\Delta\pi_{j,jp,t}^{p_{j,jp}}|} \tag{5.24}$$

$$\delta_{j,jp}^{p_{j,jp}+1} \le y_{j,jp}^{p_{j,jp}} \le \delta_{j,jp}^{p_{j,jp}} \quad \forall p_{j,jp} \in P_{j,jp} - 1 \tag{5.25}$$

$$0 \le \delta_{j,jp}^{p_{j,jp}} \le 1, \quad y_{j,jp}^{p_{j,jp}} \ binary \quad \forall p_{j,jp} \in P_{j,jp} \tag{5.26}$$

5.3 Electric Power System Model

5.3.1 Electric power system model assumptions

Similar to the natural gas system model, the costs in the electric power system model include

penalties for unmet electric power demand, generators' start-up and shut-down costs. Start-up

cost is the dollars per start composed by the start-up fuel cost, station service cost, start

maintenance adder and addition starting labor cost. No load cost is the total cost of maintaining

those zero net output generators' synchronous speed. The incremental energy cost for a unit is

defined as the resources' variable cost per megawatt-hour which does not include the no-load

cost.

According to the definition of no-load cost and incremental energy cost, the fuel cost takes

account of the principal part of the no-load cost and incremental cost. And for an integrated

natural gas and electric power system, those fuel costs of gas fueled power generators has already been taken into account in the gas exploration process.

On the constraint aspect, for each node, a dynamic equilibrium constraint of electric power is crucial for each hour, in which the whole electric demand plus the net electric inflow and non-served electricity are required to be identical with the electric supply from wind and natural gas. Moreover, a status of on (off) is given to those generators started up (shut down) already or being started up (shut down). Here we assume the gas fueled power generators only require one hour to start up or shut down, and the cost of starting up or shutting down is a given parameter. What's more, for each natural gas fueled generator, there is one upper bound and lower bound for the production level, ramp rate, on or off time and reserves. Also, we assume all those reserves come from the gas fueled power generators. The operational cost of wind turbines is considered negligible. For power transmission lines, under the assumptions of DC power flow and neglecting reactive power and resistance of transmission lines, the power flow could be described by voltage angle gap and reactance, while all voltage magnitudes equal to one p.u. and all angles are small.

5.3.2 Electric power system model

The following part is the formulation of electric power system optimization model:

- *Objective function*: Minimize the total cost of the electric power system includes start-up cost, shut-down cost, non-served electricity penalties and non-served reserve penalties. For the no-load cost and incremental cost, the principal component of them is the cost of fuel which has already been taken into account in the gas system.

$$\min\left\{\sum_{t=1}^{24}\left[\sum_{ug\in UG}C_{ug}^{SU}su_{ug,t}+\sum_{ug\in UG}C_{ug}^{SD}sd_{ug,t}+\sum_{i\in I}C_i^{NSP}nsp_{i,t}+C^{NSR}nsr_t\right]\right\} \tag{5.27}$$

- *Power flow equilibrium constraints:* For each node in the electric power system, at each hour, there is a balance between the power supply from gas fueled power generators and wind power plants, non-served electricity, power demand and power flow into and out of this node.

$$\sum_{ug\in UG(i)}gpp_{ug,t}+\sum_{uw\in UW(i)}wpp_{uw,t}+nsp_{i,t}\geq PD_{i,t}^{pred}+\sum_{ip\in c_I(i)}pf_{i,ip,t} \quad \forall i\in I,\forall t\in T \tag{5.28}$$

- *Generator start-up and shut-down constraints*: Eq. (5.29) states that with the assumption of one hour start-up or shut-down process, if a generator is started up (shut down) in hour t, then it must be off (on) one hour before and $su_{ug,t}=1, sd_{ug,t-1}=0, u_{ug,t}=1, u_{ug,t-1}=0$ ($su_{ug,t}=0, sd_{ug,t-1}=1, u_{ug,t}=0, u_{ug,t-1}=1$). Eq. (5.30) is the boundary condition for Eq. (5.29), while (5.31) and (5.32) assert that once a generator is started up (shut down) respectively, it will be in the on (off) state in that hour. Moreover, Eq. (5.33) states that in any hour, at most one of the starting up and shutting down processes will happen.

$$u_{ug,t}-u_{ug,t-1}=su_{ug,t}-sd_{ug,t-1} \quad \forall ug\in UG,\forall t\in\{2,3,...,24\} \tag{5.29}$$

$$u_{ug,1}-U_{ug}^{initial}=su_{ug,1}-SD_{ug}^{initial} \tag{5.30}$$

$$u_{ug,t}\geq su_{ug,t} \quad \forall ug\in UG,\forall t\in T \tag{5.31}$$

$$u_{ug,t}\leq 1-sd_{ug,t} \quad \forall ug\in UG,\forall t\in T \tag{5.32}$$

$$su_{ug,t}+sd_{ug,t}\leq 1 \quad \forall ug\in UG,\forall t\in T \tag{5.33}$$

- *Maximum and minimum generation*: The following points are simultaneously addressed by Eq. (5.34).

➢ If power generator is being started up which means $u_{ug,t} = 1, su_{ug,t} = 1, sd_{ug,t} = 0,$

then $(gpp_{ug,t} + r_{ug,t}) \in \left[0, \underline{GPP_{ug}}\right].$

➢ If power generator is being shut down which means $u_{ug,t} = 1, su_{ug,t} = 0, sd_{ug,t} = 1,$ then $(gpp_{ug,t} + r_{ug,t}) \in \left[0, \underline{GPP_{ug}}\right].$

➢ If power generator is on and neither being started up or shut down which $u_{ug,t} = 1,$ $su_{ug,t} = 0, sd_{ug,t} = 0,$ then $(gpp_{ug,t} + r_{ug,t}) \in \left[\underline{GPP_{ug}}, \overline{GPP_{ug}}\right].$

$$0 \le gpp_{ug,t} + r_{ug,t} \le \overline{GPP_{ug}} u_{ug,t} - su_{ug,t}(\overline{GPP_{ug}} - \underline{GPP_{ug}}) - sd_{ug,t}(\overline{GPP_{ug}} - \underline{GPP_{ug}})$$
$$\forall ug \in UG, \forall t \in T \tag{5.34}$$

$$gpp_{ug,t} \ge \underline{GPP_{ug}^P} u_{ug,t} - \underline{GPP_{ug}^P} su_{ug,t} - \underline{GPP_{ug}^P} sd_{ug,t} \quad \forall ug \in UG, \forall t \in T \tag{5.35}$$

- *Reserve limit:* Eq. (5.36) and (5.37) express the upper and lower bounds of the reserves, in which we assume all those reserves come from the gas fueled power generators.

$$r_{ug,t} \le \left[\overline{GPP_{ug}} u_{ug,t} - (\overline{GPP_{ug}} - \underline{GPP_{ug}}) su_{ug,t} - (\overline{GPP_{ug}} - \underline{GPP_{ug}}) sd_{ug,t}\right] MAXSP_{ug} \tag{5.36}$$
$$\forall ug \in UG, \forall t \in T$$

$$\sum_{ug \in UG} r_{ug,t} + nsr_t = WR_t \sum_{uw \in UW} \overline{WPP_{uw,t}} \quad \forall t \in T \tag{5.37}$$

- *Ramp up and down constraints: Eq. (5.38) and (5.39) denote that the change in production of a natural gas fueled power generator in two consecutive hours is bounded.*

$$-RD_{ug} \le gpp_{ug,t} - gpp_{ug,t-1} \le RU_{ug} \quad \forall ug \in UG, \forall t \in \{2,3,...,24\} \tag{5.38}$$

$$-RD_{ug} \le gpp_{ug,1} - GPP_{ug}^{initial} \le RU_{ug} \quad \forall ug \in UG \tag{5.39}$$

- *Minimum on and off time:* Eq. (5.40) and (5.41) indicate that once a generator is on (off), it is required to be on (off) for some number of hours.

$$\sum_{tt=t-TU_{ug}+1}^{t} su_{ug,t} \leq u_{ug,t}, \ \forall ug \in UG, \forall t \in \{TU_{ug},\ldots,24\} \tag{5.40}$$

$$\sum_{tt=t-TD_{ug}+1}^{t} sd_{ug,t} \leq 1-u_{ug,t}, \forall ug \in UG, \forall t \in \{TD_{ug},\ldots,24\} \tag{5.41}$$

- *Wind power capacity:* The wind energy output is bounded by the current wind energy available for each hour.

$$wpp_{uw,t} \leq \overline{WPP_{uw,t}} \quad \forall uw \in UW, \forall t \in T \tag{5.42}$$

- *Transmission line constraints:* The power flow from one node to another could be described as Eq. (5.43), and Eq. (5.44) gives upper and lower bound for power flow.

$$pf_{i,ip,t} = \frac{\theta_{i,t} - \theta_{ip,t}}{X_{i,ip}}, \ \forall ip \in c_{I(i)}, \forall i \in I \tag{5.43}$$

$$-\overline{PF_{i,ip}} \leq pf_{i,ip,t} \leq \overline{PF_{i,ip}}, \ \forall ip \in c_{I(i)}, \forall i \in I \tag{5.44}$$

5.4 Combined Deterministic MILP Model

- *Connection:* Natural gas fueled power generators form the connections between the natural gas system and the electric power system. We assume the amount of gas they consume is a linear function of the power output. Then we only need to add one constraint to calculate the amount of gas required to produce electricity, where Bf_{ug} and Cf_{ug} are slope and intercept parameters of gas consuming function for each gas fueled power generator.

$$egd_{ug,t} = Bf_{ug} gpp_{ug,t} + Cf_{ug} \tag{5.45}$$

5.5 Three Models for Comparison

In order to compare the deterministic optimization problem and the stochastic optimization problem, here we introduce three models.

5.5.1 Wait and see model

For the wait and see model, the decision maker makes no decisions until the values of all random parameters $\overline{WPP_{uw,t}}$ are realized. In other words, for each scenario, the decision maker will know the exact value of random variables and then make a decision on all variables. Because we know the exact value of the wind energy output for each scenario, we don't require the reserve variables any more or we can set them to be zero.

Given the specific wind energy output for each scenario, a specific deterministic model is solved with reserves set to be zero. All variables' optimal values and the optimal objective value depend on scenarios. The objective function for scenario s could be described as $\xi^{WS,s}$ for the wait and see model and the constraints for each scenario are similar to the deterministic optimization model. The optimal objective value of the wait and see model is $\sum_{s \in S} Prob^s \xi^{WS,s}$. The optimal value of the wait and see model forms a lower bound on the optimal cost of the stochastic optimization problem.

$$\xi^{WS,s} = Min \left\{ \begin{array}{l} \displaystyle\sum_{ug \in UG} C_{ug}^{SU} su_{ug,t}^{s} + \sum_{ug \in UG} C_{ug}^{SD} sd_{ug,t}^{s} + \sum_{w \in W} C_{w}^{G} gp_{w}^{s} \\[2em] + \displaystyle\sum_{t=1}^{24} \left[\begin{array}{l} \displaystyle\sum_{i \in I} C_{i}^{NSP} nsp_{i,t}^{s} + \sum_{stor \in STOR} C_{stor,t}^{STOR} \times q_{stor,t}^{OUT,s} \\[1.5em] + \displaystyle\sum_{j \in J} C_{j}^{NSG} nsg_{j,t}^{s} + C^{NSR} nsr_{t}^{s} \end{array} \right] \end{array} \right\} \tag{5.46}$$

5.5.2 Deterministic model with reserves

Adding some reserves to the power supply is a widely used method to alleviate the wind energy uncertainty. This is exactly what we have done in the deterministic optimization model. In the day-ahead market, given the wind energy forecast data, the deterministic optimization model is applied to find the optimal solution:

$$\left[\begin{array}{l} gp_{w}^{*}, \pi_{j,t}^{*}, \Delta\pi_{j,jp,t}^{*}, gf_{j,jp,t}^{*}, su_{ug,t}^{*}, sd_{ug,t}^{*}, u_{ug,t}^{*}, \delta_{j,jp}^{*p_{j,jp}}, y_{j,jp}^{*p_{j,jp}} \\ gpp_{ug,t}^{*}, wpp_{ug,t}^{*}, q_{stor,t}^{OUT*}, q_{stor,t}^{IN*} level_{stor,t}^{*}, nsp_{i,t}^{*}, nsg_{j,t}^{*}, egd_{ug,t}^{*}, pf_{i,ip,t}^{*}, nsr_{t}^{*}, gr_{ug,t}^{*} \end{array} \right]$$

With an objective to evaluate how well the first stage variables' solutions are and compare the deterministic model with reserves and the two-stage stochastic optimization model, all those first stage variables are fixed to be the optimal value.

$$\left[gp_{w}, \pi_{j,t}, \Delta\pi_{j,jp,t}, gf_{j,jp,t}, su_{ug,t}, sd_{ug,t}, u_{ug,t}, \delta_{j,jp}^{p_{j,jp}}, y_{j,jp}^{p_{j,jp}} \right]$$

$$= \left[gp_{w}^{*}, \pi_{j,t}^{*}, \Delta\pi_{j,jp,t}^{*}, gf_{j,jp,t}^{*}, su_{ug,t}^{*}, sd_{ug,t}^{*}, u_{ug,t}^{*}, \delta_{j,jp}^{*p_{j,jp}}, y_{j,jp}^{*p_{j,jp}} \right]$$

And then under each scenario, we solve deterministic optimization with specific wind energy and no reserves: $\left[gpp_{ug,t}^{s}, wpp_{ug,t}^{s}, q_{stor,t}^{OUT,s}, q_{stor,t}^{IN,s} level_{stor,t}^{s}, nsp_{i,t}^{s}, nsg_{j,t}^{s}, egd_{ug,t}^{s}, pf_{i,ip,t}^{s} \right]$ and decide the corresponding optimal objective value for each scenario $\xi^{DR,s}$. The final objective value for this model is $\displaystyle\sum_{s \in S} Prob^{s} \xi^{DR,s}$.

5.5.3 Here and now model: Combined two-stage stochastic MILP model

The deterministic model is formulated with fixed energy reserves, whereas wind power

forecasting is one of the most variable and unpredictable tasks. The stochastic unit commitment

and gas network scheduling problem is developed to utilize the two-stage stochastic optimization

approach and thus maintain the combined system's reliability. In this two-stage stochastic

optimization model, the first stage will decide the unit commitment solution of the power system

and gas production and scheduling of natural gas network simultaneously, and the power

dispatch decisions and natural gas storage facilities' schedule will made given various scenarios,

considering the natural gas transmission process is a time-consuming process compared with the

electric transmission and constancy of gas supply in gas wells. Specifically, in the first stage, a

decision on the natural gas output in gas wells, pressure squared and pressure square gap in each

node and corresponding gas flow in pipelines in natural gas system will be made, as well as the

unit commitment decisions for power system. Also, all those variables involved in the

approximation process of gas flow in pipelines, $\delta_{j,jp}^{p_{j,jp}}$ and $y_{j,jp}^{p_{j,jp}}$, are assigned to be in the first

stage. In the second stage, the real-time hourly power generation from wind and gas, the gas flow

into or out of storage facilities, storage facilities' hourly storage level, and all those variables

about the dispatch process of electricity will be decided. In addition, reserve limits are set to zero

because we already consider various scenarios by applying stochastic optimization model.

- First stage variables: gp_w, $\pi_{j,t}$, $\Delta\pi_{j,jp,t}$, $gf_{j,jp,t}$, $su_{ug,t}$, $sd_{ug,t}$, $u_{ug,t}$, $\delta_{j,jp}^{p_{j,jp}}$, $y_{j,jp}^{p_{j,jp}}$

- Second stage variables:

  $gpp_{ug,t}^s$, $wpp_{ug,t}^s$, $q_{stor,t}^{OUT,s}$, $q_{stor,t}^{IN,s}$ $level_{stor,t}^s$, $nsp_{i,t}^s$, $nsg_{j,t}^s$, $egd_{ug,t}^s$, $pf_{i,ip,t}^s$

  The two–stage stochastic formulation is as follows:

- *Objective function:* Minimize total cost of the unit commitment and gas wells production cost in the first stage and the expected value of generating cost, gas cost from storage facilities, non-served power and gas cost and non-served reserve cost in the second stage.

$$Min \left\{ \begin{array}{l} \left[\sum_{ug \in UG} C_{ug}^{SU} su_{ug,t} + \sum_{ug \in UG} C_{ug}^{SD} sd_{ug,t} + \sum_{w \in W} C_w^G gp_w \right. \\ \left. + \sum_{s \in S} Prob^s \sum_{t=1}^{24} \left[\begin{array}{l} \sum_{i \in I} C_i^{NSP} nsp_{i,t}^s + \sum_{stor \in STOR} C_{stor,t}^{STOR} \times q_{stor,t}^{OUT,s} \\ + \sum_{j \in J} C_j^{NSG} nsg_{j,t}^s + C^{NSR} nsr_t^s \end{array} \right] \end{array} \right\}$$

- *Constraints:* All those constraints that only include the first stage variables are assigned as the first stage constraints, and all those constraints including at least one second stage variables are assigned to be the second stage constraints. The complete formulation of the two-stage stochastic optimization model for the combined natural gas and power system including wind energy is listed in the Appendix.

CHAPTER 6. CASE STUDY

In this section, a single day case study is formulated and the corresponding data are listed. Numerical results are presented for the deterministic optimization problem with the forecasted hourly wind power output distribution and the two-stage stochastic optimization model for various hourly wind power output distribution scenarios for one day. Most of the data comes from a six-bus power with seven-node gas system (Liu et al., 2009).

6.1 Assumptions and data
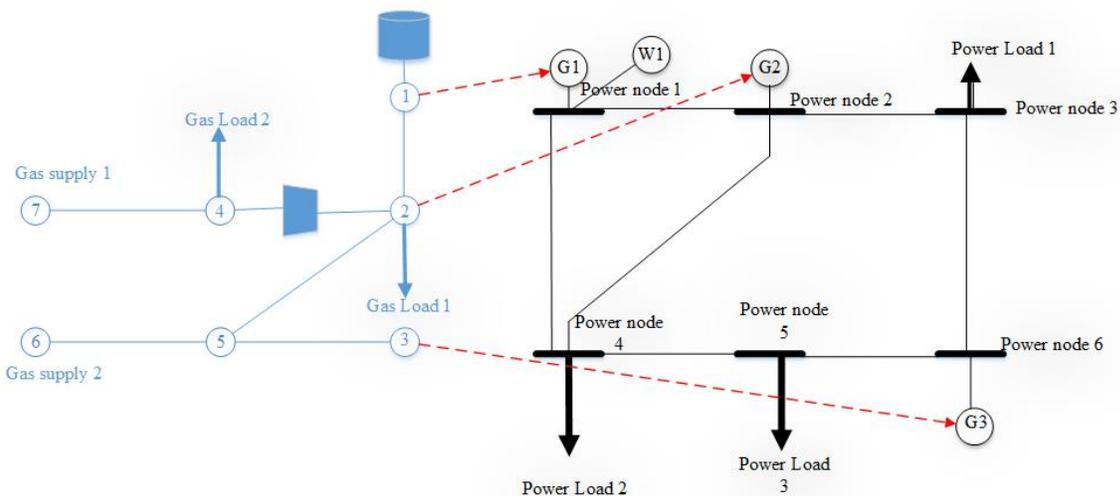
Figure 14 A six-bus power with seven-node gas system

As listed in Figure 14, we use bars to represent the electric system, circles to represent gas system and dashed arrowed lines to show the connections of electric system and gas system. Three natural gas fueled power generators are located in power node 1, 2 and 6 separately and there is one wind power generator in power node 1. Power load exists in load 3, 4 and 5 taking

account of 20, 40 and 40 percent of the hourly gross power load. Seven transmission lines connect the power nodes. For the natural gas network, each of nodes 6 and 7 has one gas supplier (well). There exists one gas storage facility in gas node 1. One compressor and five passive pipelines connect the gas nodes. Assume the compressor is located at the middle of the active pipeline and the three red arrowed lines connecting natural gas system and power system illustrate which gas node is supplying the non-electric gas demand in the gas fueled power generators.

6.1.1 Natural gas system data

The maximum and minimum pressure and penalties of non-served gas for each gas node are listed in Table 1. Table 2 lists the maximum and minimum daily gas output and supply cost for each gas well. Table 3 shows the relevant data of the storage facilities including the index identifying storage facilities and gas node, maximum and minimum storage level, maximum flow rate, initial storage level and storage cost. Table 4 and 5 include the indexes and parameters of passive pipelines and compressor stations respectively. Furthermore, hourly gross non-electric gas demand is 6000 kcf/hour, divided into gas node 2 and 4 with the ratio of 2 to 1. Here we assume 1 kcf of natural gas can generate 1 MBtu of energy.

Table 1 Gas node data

Gas Node No., j	Min Pressure, $\underline{pr_j}$ (Psig)	Max Pressure, $\overline{pr_j}$ (Psig)	Non-Served Gas Cost, C_j^{NSG} ($/kcf)
1	105	150	3500
2	140	170	3500
3	150	195	3500

4	70	100	3500
5	150	200	3500
6	160	240	3500
7	100	140	3500

Table 2 Data of gas suppliers

No., w	Gas Node No., j	Min-Output, $\underline{GP_w}$ (kcf/day)	Max-Output, $\overline{GP_w}$ (kcf/day)	Supply Cost, C_w^G ($/MBtu)
1	6	0	63600	1.68
2	7	0	72000	2.28

Table 3 Data of storage facilities

No., $stor$	Gas Node No., j	Max-Level, $\overline{Cap_{stor}}$ (kcf)	Min-Level, $\underline{Cap_{stor}}$ (kcf)	Max-Flow Rate, Q_{stor} (kcf/h)	Ini-Level, $LEVEL_{stor}^{initial}$ (kcf)	Storage Cost, C_{stor}^{STOR} ($/kcf)
1	1	15000	5000	2000	15000	3

Table 4 Data of passive pipelines

Pipeline Index	From Node, j	To Node, pjp	$C_{j,jp}$ (kcf/Psig)
1	1	2	50.6
2	2	5	37.5
3	5	6	45.3
4	3	5	43.5
5	4	7	50.1

Table 5 Compressors data

Pipeline Index	From Node, j	To Node, ajp	$C_{j,ajp}^{right}$ (kcf/Psig)	$C_{j,ajp}^{left}$ (kcf/Psig)	$\tau_{j,ajp}$
6	2	4	100.2	100.2	1.15

6.1.2 Electric power system data

Tables 6, 7 and 8 list the parameters of power nodes, gas fueled power generators and power transmission lines, respectively. Predicted hourly gross electric loads are illustrated in Table 9 and Figure 15. The electric load would be divided among power node 1, 2 and 3 with the ratio of 1:2:2. We set the maximum spinning reserve for each generator $MAXSP_{ug}$ to be 0.3. And the reserve margin for wind power WR_t is set according to the ratio of wind forecast and electric load (Jin et al., 2014).

Table 6 Data of power node

Node No., i	Non-served power cost, C_i^{NSP} ($/MW$)	Non-served reserve cost, C_i^{NSR} ($/MW$)
1	3500	1100
2	3500	1100
3	3500	1100
4	3500	1100

Table 7 Data of gas fueled power generators

Unit, ug	1	2	3
Power Node	1	2	6
Gas Node	1	2	3
$GPP_{ug}^{initial}$ (MW)	150	50	0
$\overline{GP_{ug}}$ (MW)	100	10	10
$\underline{GP_{ug}}$ (MW)	220	100	20
MaxRampUp, RU_{ug} (MW/h)	55	50	20
MaxRampDown, RD_{ug} (MW/h)	55	50	20
MinOn, TU_{ug} (hours)	4	2	1
Minoff, TD_{ug} (hours)	4	3	1

	4	2	0
IniOnHour, $TU_{ug}^{initial}$ (hours)	4	2	0
IniOffHour, $TD_{ug}^{initial}$ (hours)	0	0	1
Bf (MBtu /MWh)	13.51	32.63	17.7
Cf (MBtu/h)	176.95	129.97	137.41
$U_{ug}^{initial}$	1	1	0
$SU_{ug}^{initial}$	0	0	0
$SD_{ug}^{initial}$	0	0	0
C_{ug}^{SU} (\$/h)	0	0	0
C_{ug}^{SD} (\$/h)	0	0	0

Table 8 Transmission lines data

Line No.	From Bus, i	To Bus, ip	Reactance, $X_{i,ip}$ (p.u.)	Power Flow Limit, $\overline{PF_{i,ip}}$ (MW)
1	1	2	0.170	200
2	1	4	0.258	100
3	2	4	0.197	100
4	5	6	0.140	100
5	2	3	0.037	100
6	4	5	0.037	100
7	3	6	0.018	100

Table 9 Predicted hourly gross electricity load data for one day

| Hour	Load, PD_t^{pred} (MW)	Hour	Load, PD_t^{pred} (MW)	Hour	Load, PD_t^{pred} (MW)
1	175.19	9	205.56	17	256.00
2	165.15	10	217.20	18	246.74
3	158.67	11	228.61	19	235.97
4	154.73	12	236.1	20	237.35
5	155.06	13	242.18	21	237.31
6	160.48	14	243.60	22	227.14
7	173.39	15	248.86	23	201.05
8	190.40	16	255.79	24	196.75
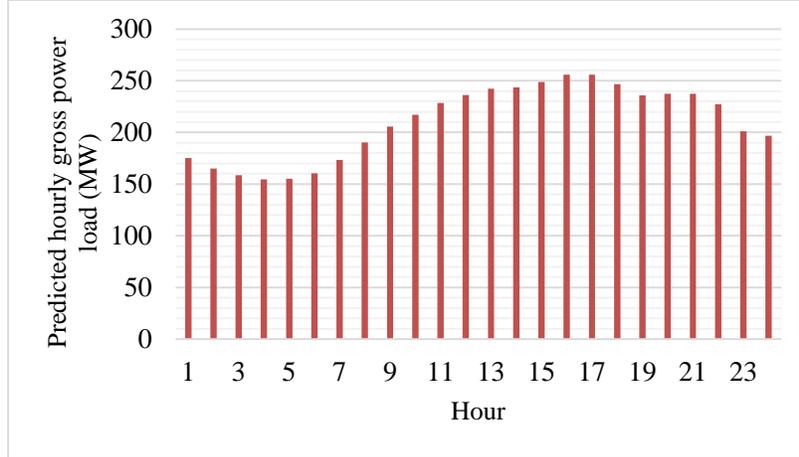
Figure 15 Predicted hourly gross power load

6.1.3 Wind power scenario generation

The scenario generation on the basis of a quantile regression method is applied (Sari et al., 2015). One day ahead of the real time market, hourly wind power for one wind power plant is projected and day-ahead wind power forecast (DWPF) is expressed as:

$$\overline{wpp}_{uw,t} = \left(\overline{wpp}_{uw,1}, \overline{wpp}_{uw,2}, ..., \overline{wpp}_{uw,24} \right)$$

while in the real time market, real wind power is obtained as:

$$wpp_{uw} = \left(wpp_{uw,1}, wpp_{uw,2}, ..., wpp_{uw,24} \right)$$

The corresponding day-ahead wind power forecast error (DWPFE) is

$$e_{uw} = \left(e_{uw,1}, e_{uw,2}, ..., e_{uw,24} \right),$$

in which $e_{uw,t} = \overline{wpp}_{uw,t} - wpp_{uw,t}$. The quantile regression method assumes that actual wind power output, DWPF and DWPFE are normalized by wind power capacity and then find the cumulative distribution of the sampled DWPFE given DWPF. And then the DWPFE distribution is used to find the quantile values of $e_{uw,t}^{*}$ by applying linear interpolation to the set of quantiles.

Once the quantile values are found, the natural cubic spline with three basic functions is applied

to connect a quantile of forecast error and DWPF nonlinearly. Then the wind scenarios could be

found by subtracting the forecast error from DWPF. Sari (2015) generated twenty-seven equally

likely scenarios for hourly wind output distribution in each day for a year. Figure 28 illustrates

the actual wind supply and wind forecast in one day.

6.2 Experiment Results

6.2.1 Daily average cost and sample standard deviation analysis

We have the wind power hourly distribution forecast and observational value for 339 days in

one year. If we use $x_d^s = (u_d^s, v_d^s)$ and $f(x_d^s)$ to represent the optimal solution and objective

value of each scenario in which u_d^s is the solution to the first stage variables and v_d^s is the

solution to the second stage variables. Then the daily average cost and the sample standard

deviation of cost are expressed as:

$$E_d = \sum_{s \in S} Prob^s f(x_d^s) \tag{6.1}$$

$$\sigma_d = \sqrt{\sum_{s \in S} Prob^s \left[f(x_d^s) - E_d \right]^2} \tag{6.2}$$

We use E_d^{WS}, E_d^{HN}, E_d^{DR} and σ_d^{WS}, σ_d^{HN}, σ_d^{DR} respectively to represent the average cost and

the sample standard deviation of cost for wait and see, here and now models and deterministic

model with reserves. In addition, we could find the overall expected value of the daily average

cost and the daily sample standard deviation for the 339 days by using Eq. (6.3), (6.4) and (6.5).

Table 10 compares the expected value for the daily average cost and the daily sample standard

deviation of cost and illustrates that the wait and see model has the best expected daily average

cost, while the here and now model has the best expected sample standard deviation.

$$\overline{E^{WS}} = \frac{1}{339}\sum_{d=1}^{339} E_d^{WS}, \overline{\sigma^{WS}} = \frac{1}{339}\sum_{d=1}^{339} \sigma_d^{WS} \qquad (6.3)$$

$$\overline{E^{HN}} = \frac{1}{339}\sum_{d=1}^{339} E_d^{HN}, \overline{\sigma^{HN}} = \frac{1}{339}\sum_{d=1}^{339} \sigma_d^{HN} \qquad (6.4)$$

$$\overline{E^{DR}} = \frac{1}{339}\sum_{d=1}^{339} E_d^{DR}, \overline{\sigma^{DR}} = \frac{1}{339}\sum_{d=1}^{339} \sigma_d^{DR} \qquad (6.5)$$

Table 10 Expected value of daily average cost and the sample standard deviation

Model	Mean daily cost, $\overline{E}(\$)$	Mean sample standard deviation of daily cost, $\overline{\sigma}(\$)$
WS	434,834	5,434
HN	436,391	5,024
DR	448,424	36,893

Table 11 lists the comparison result of the daily sample standard deviation for these three models, from which we can tell that the here and now model has the highest frequency of having the smallest sample standard deviation. Figures 16 and 17 illustrate the frequency distribution for each average daily cost and daily cost sample standard deviation.

Table 11 Daily sample standard deviation of cost comparison for three models

|	No. of days	Percentage
$\sigma_d^{WS} < \sigma_d^{HN}$ and $\sigma_d^{WS} < \sigma_d^{DR}$	29	0.086
$\sigma_d^{HN} < \sigma_d^{WS}$ and $\sigma_d^{HN} < \sigma_d^{DR}$	182	0.537
$\sigma_d^{DR} < \sigma_d^{WS}$ and $\sigma_d^{DR} < \sigma_d^{HN}$	128	0.378
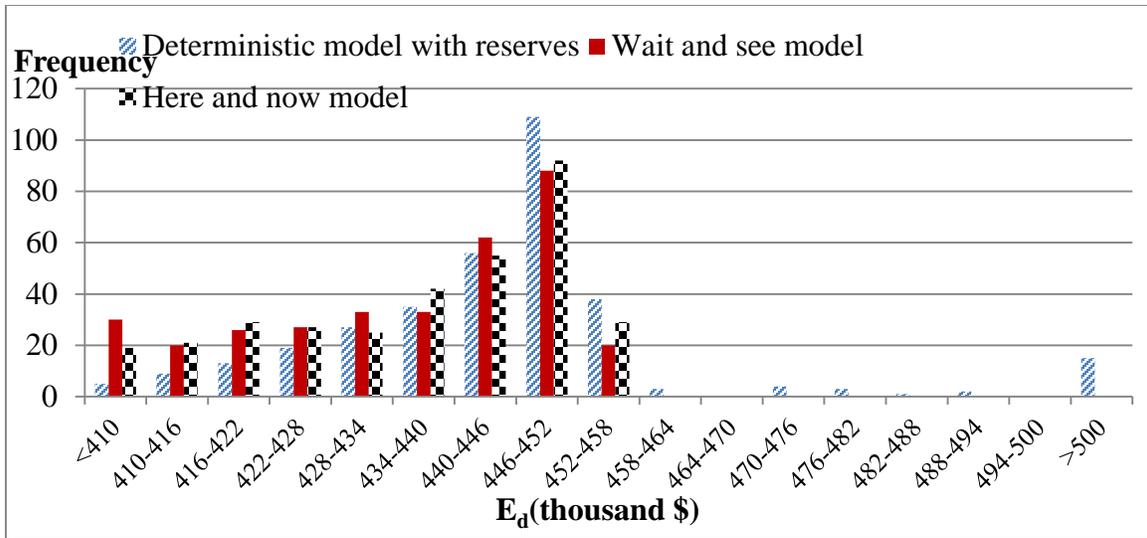
**Figure 16 Frequency for daily average cost for three models**
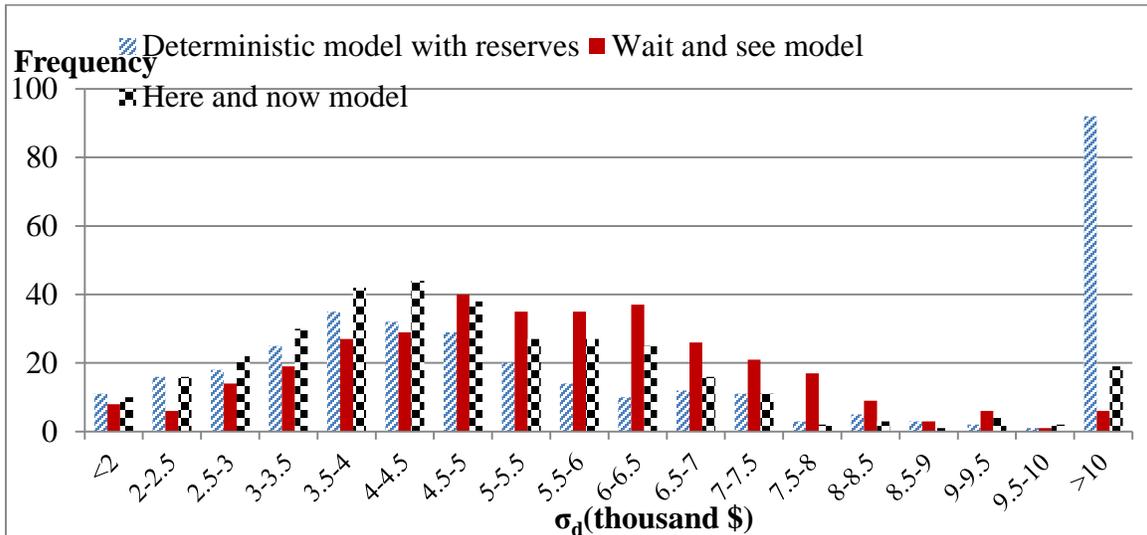
Figure 17 Frequency of daily sample standard deviation of the cost for three models

The daily average cost of those three models are illustrated in Figures 18 and 19 from which we can see the cost of here and now model is very close to the wait and see model which has the least daily average cost. And the daily average cost of the deterministic model with reserves model is close to the other two models most of the time, but in several cost peak days (e.g., day 17 and 268), the daily average cost of the deterministic model with reserves are quite large. For

each day, the wait and see model has the least optimal objective value, and the optimal objective value of the here and now model is less than the deterministic model with reserves in 286 days out of the total 339 testing days. Figures 20 and 21 illustrate the distribution of σ_d for the comparison of the three models and two models respectively. Thus, we can conclude that the here and now model has a relative low and stable cost.
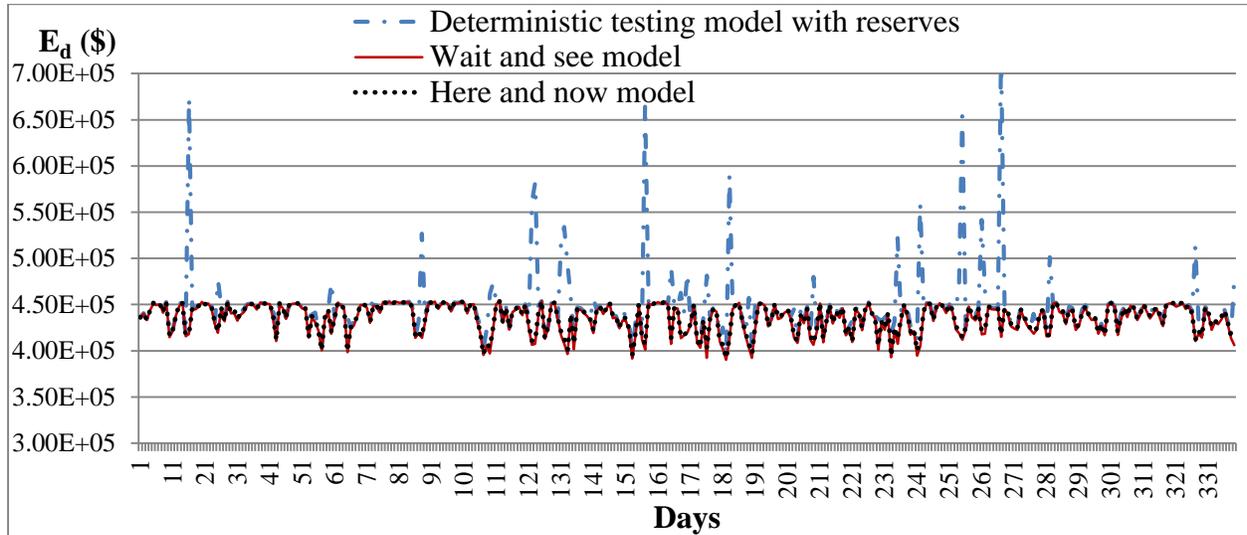


Figure 18 Daily average cost comparison of three models
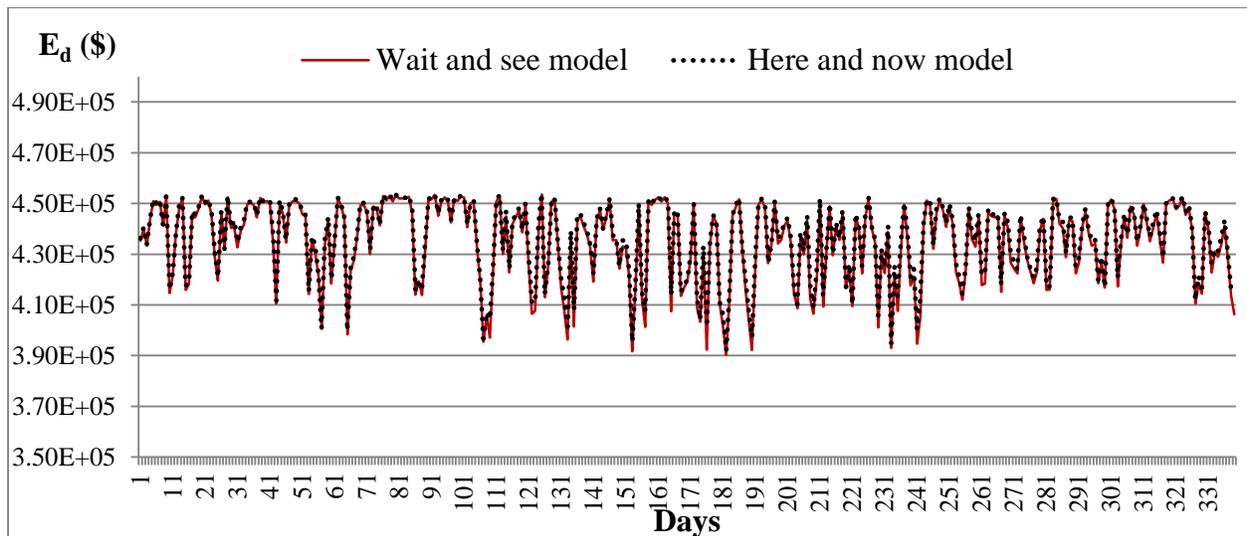
**Figure 19 Daily average cost comparison of two close models**
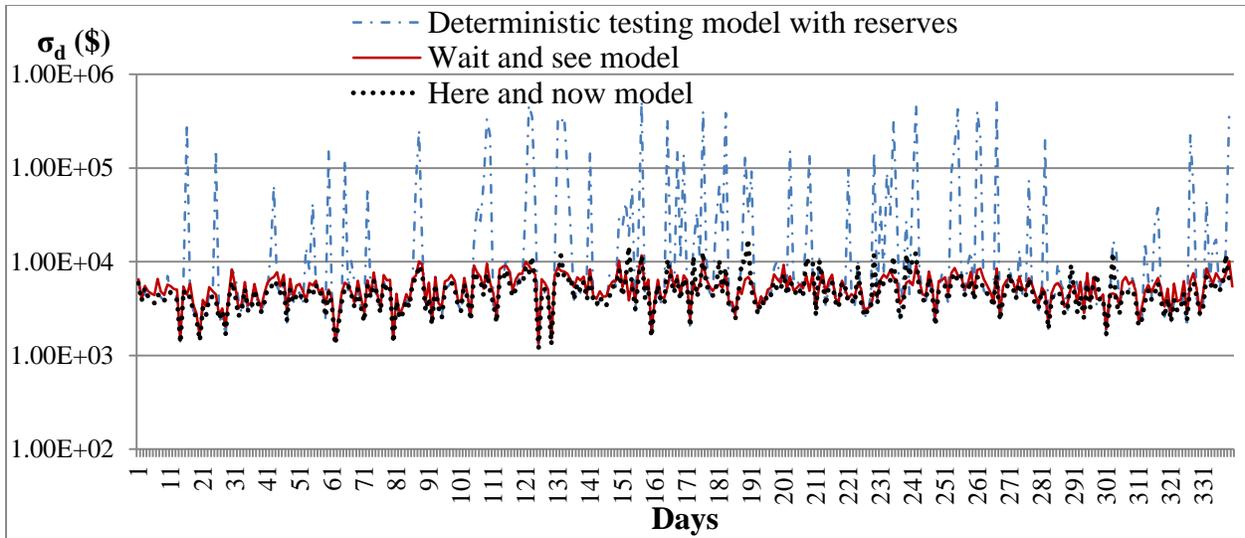
Figure 20 Comparison of daily sample standard deviation of the total cost (on log scale) for three models
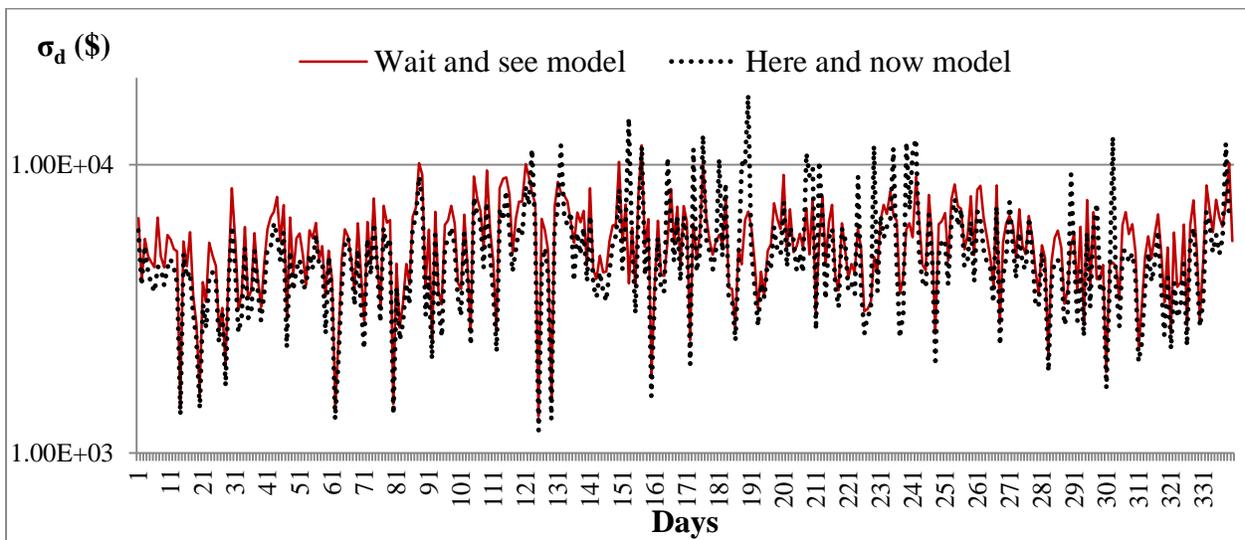
**Figure 21 Comparison of daily sample standard deviation of cost (on log scale)for two models**

6.2.2 Cost distribution analysis

Figures 22-24 illustrate the cost distribution of three models respectively. Total cost is divided into the non-served gas, non-served power, storage, and gas production costs. For all these three models, the non-served gas cost is close to zero and thus is not listed in the figure.

The cost distributions of the wait and see model and the here and now model are similar. Most of the total cost comes from gas production, taking account of almost 90 percent of the total cost, and their non-served power costs are quite small compared with the other two cost components.
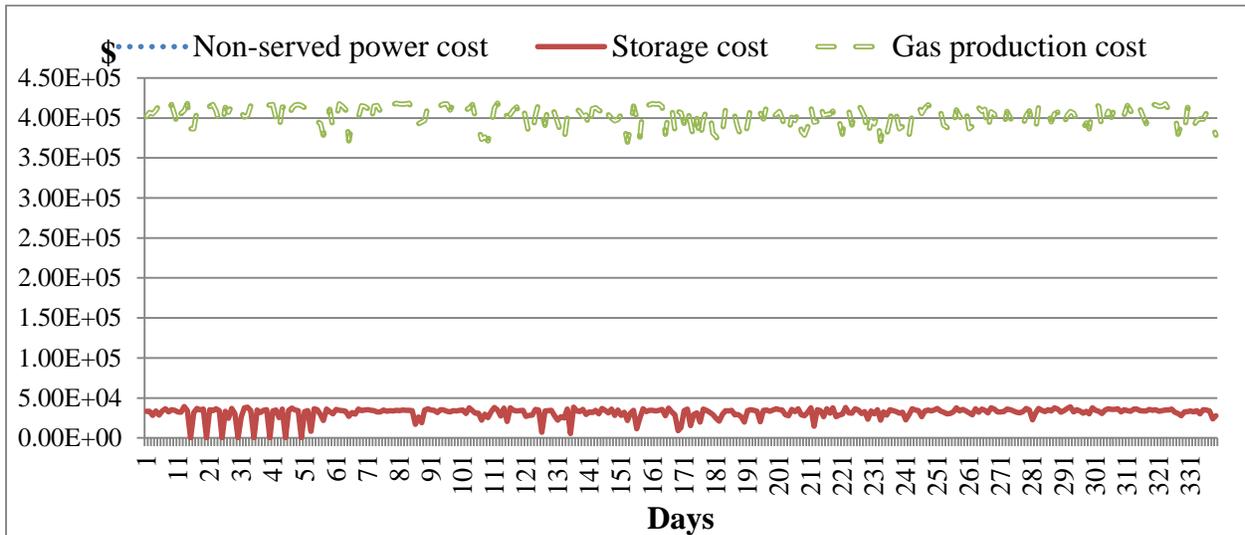

**Figure 22 Cost distribution of wait and see model**
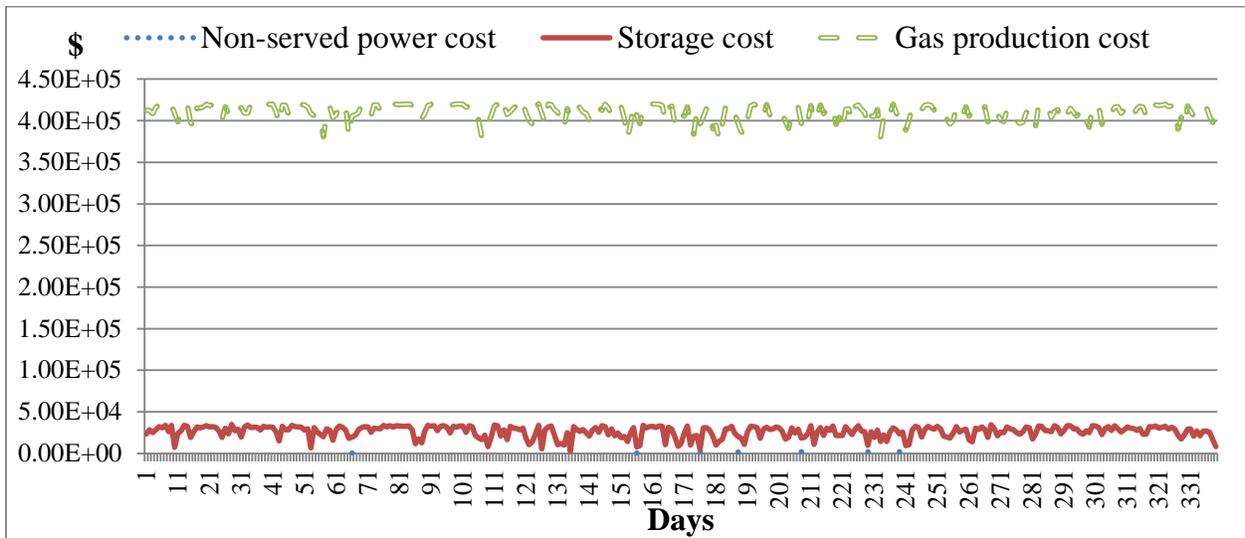
**Figure 23 Cost distribution of here and now model**
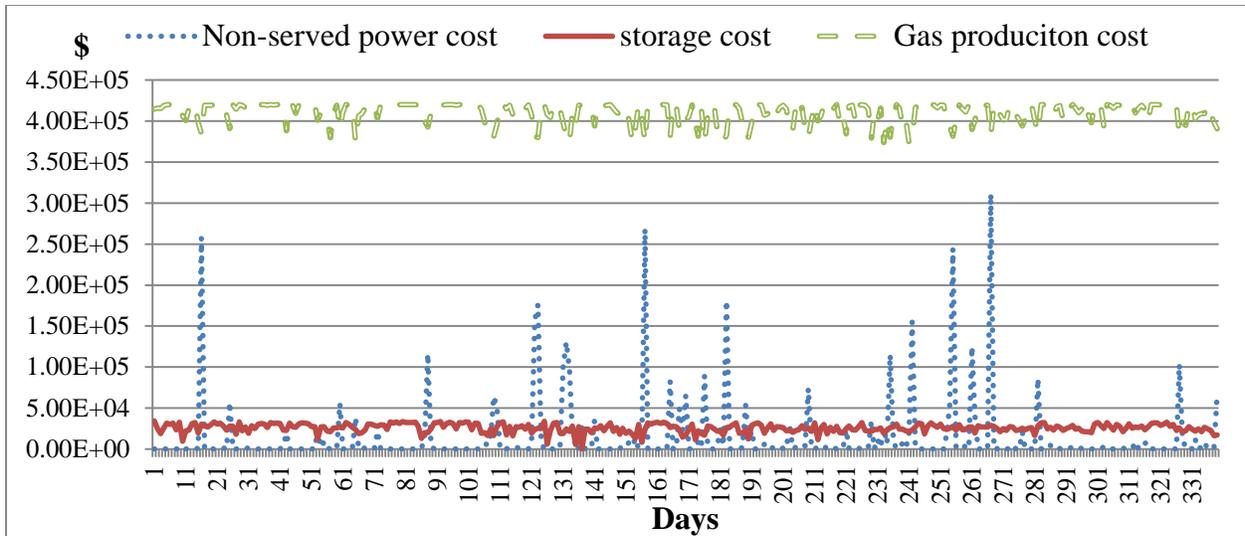
Figure 24 Cost division for deterministic model with reserves

6.2.3 System operation analysis

We pick day 157 to do analysis due to it has a very large value of the average daily cost and sample standard deviation for the deterministic testing model with reserves to help understanding the combined system operation scheme. For the here and now model and deterministic model with reserves, the decision maker makes decisions on those first-stage variables on the basis of scenario generation and wind forecast respectively. The deterministic model has some power reserves from the gas fueled power generators to compensate for the wind deficiency given the actual wind energy less than the wind energy forecast. However, once the gap between the actual wind energy and wind energy forecast reaches some limit of those reserves can compensate, the gas fueled power generators will increase the power output by using the gas from the storage facilities. Once the gas system is still not able to compensate the wind energy deficiency, then the non-served power cost will take into account. Table 12 lists some important first stage variables for the here and now and deterministic models. Both of the here and now model and the deterministic model will maintain the on status of gas fueled power generator one and two.

Furthermore, both of them will start the third gas fueled power generator at hour one under each

scenario. The specific daily gas production output for these two models at two gas wells are

given in Table 12. Figures 25-27 illustrate the cost division for various scenarios for day 157 for

three models respectively, from which we can tell that the non-served power cost is the major

factor influencing the cost of the deterministic model. And the reason is that the deterministic

model with reserves is highly dependent on the wind energy forecast, which is of high

uncertainty as well. Although the reserves can alleviate the effects of wind energy uncertainty,

the alleviation effect is limited. Once the gap between the wind forecast and actual wind energy

output is large enough, the deterministic model would have large daily average cost and sample

standard deviation.

Table 12 System operation analysis of some first stage variables for day 157

|	Here and now	Deterministic model with reserves
$u_{ug,t} \ \forall ug \in UG, \forall t \in T$	1	1
$su_{ug,1} \forall ug \in UG$	1	1
$su_{ug,t} \forall ug \in UG, \forall t \in \{2,3,...,24\}$	0	0
$sd_{ug,t} \forall ug \in UG, \forall t \in T$	0	0
gp_1 (kcf/day)	135290	126010
gp_2 (kcf/day)	76761	71471
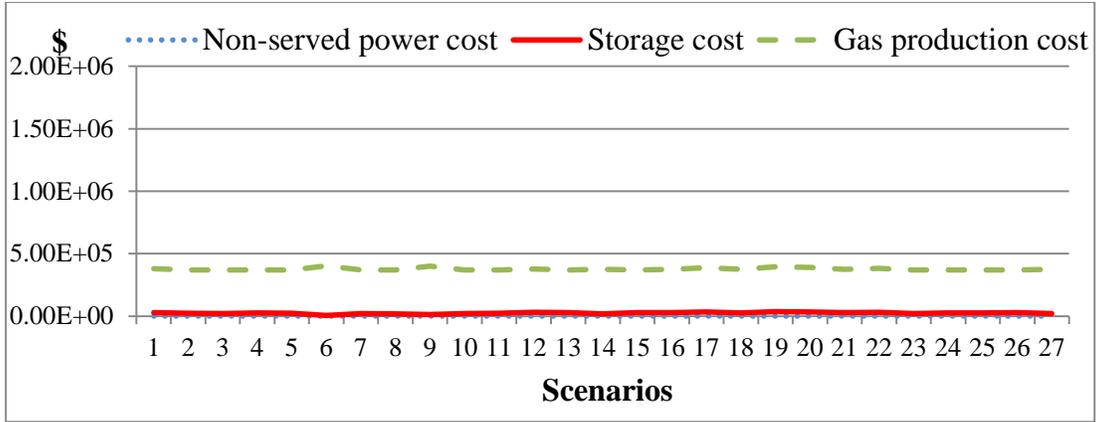
**Figure 25 Cost division of the wait and see model with reserves for day 157**
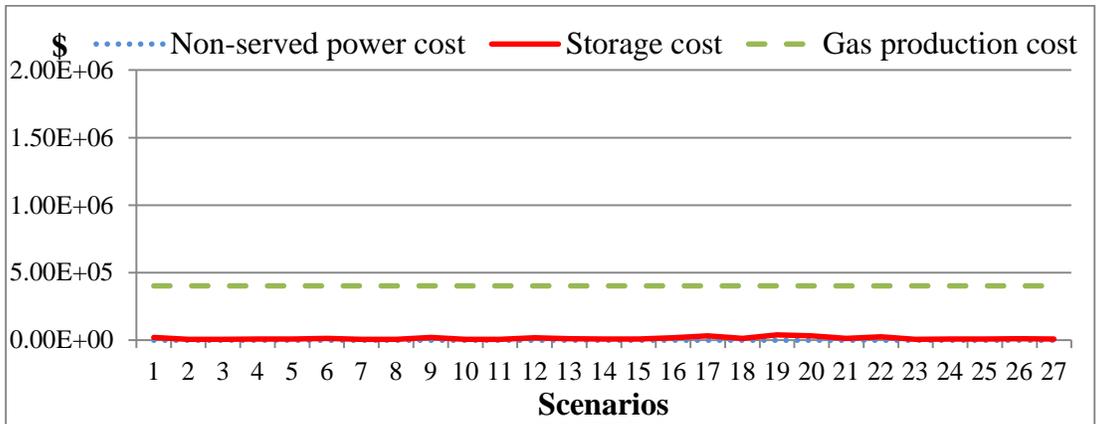
Figure 26 Cost divisions of the here and now model with reserves for day 157
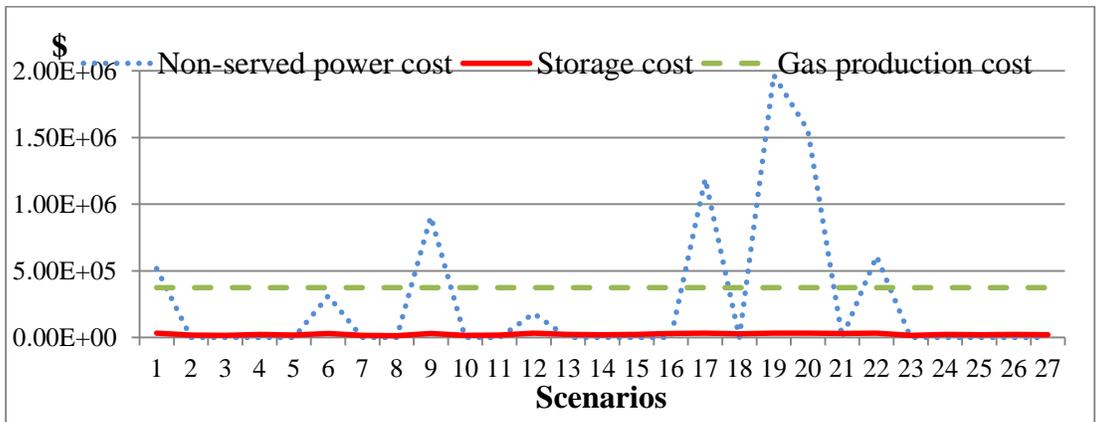
Figure 27 Cost divisions of the deterministic model with reserves for day 157

Figure 28 expresses the wind forecast and scenarios comparison for day 157. We pick

scenario 17 (dashed line in Figure 28) for further analysis. Due to in most of the 24 hours in one

day, the actual wind energy supply is less than the wind energy forecast, the total system is

required to get more gas from storage facilities to produce more power by using gas fueled

power generators. And due to the huge discrepancy, the gas from the storage facilities and the

power supply from wind and gas are not able to satisfy all the power demand, resulting in a very

huge non-served power cost in Table 13.
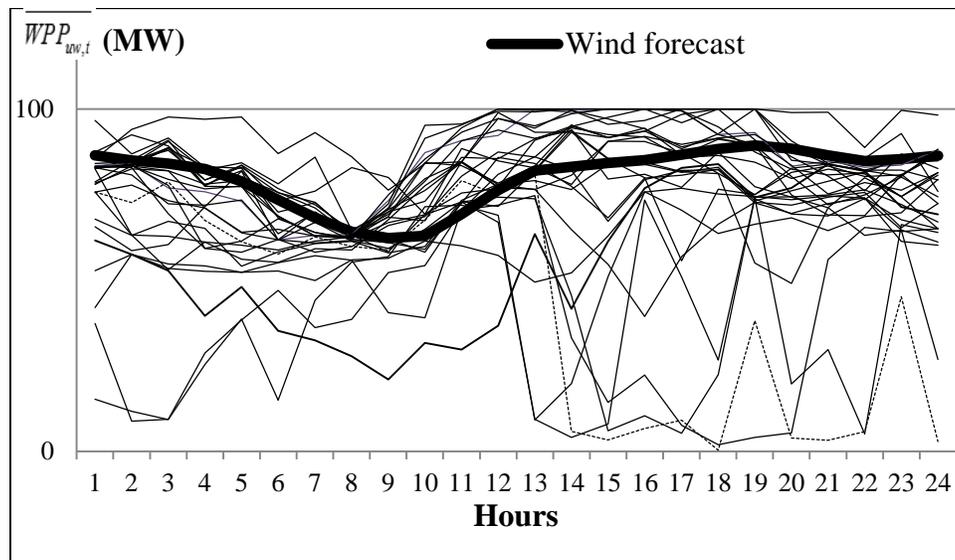
Figure 28 Wind forecast and scenarios comparison for day 157

Table 13 Daily cost analysis for day 157

Daily cost	Value ($)
Non-served gas cost	0
Non-served power cost	1191474
Gas production cost	374652
Storage cost	32190
Total cost	1598316
Total cost forecast	401580

6.2.4 Reserve margin analysis

In the previous analysis, with a given wind reserve margin, we discussed the comparison of those three models. Apart from that, we are also interested in how the reserve margin influences the result of the deterministic optimization model. Table 14 lists the results for the expected daily average cost and sample standard deviation of the daily cost for one year, in which as the wind energy reserve margin increases, the expected daily average cost first decreases and then increases, while the expected daily sample standard deviation of the cost steadily decreases. The expected daily average cost of the here and now model is less than those of all the parameter testing cases.

We pick wind reserve margin to be 0.7 which has the least expected daily average cost to do the similar analysis and compare the result with those of the three models discussed in Section 6.2.3. Figures 29 and 30 compare the daily average cost and standard deviation distributions for those three models and the deterministic optimization model with reserve margin being 0.7. Most of the daily average costs of the deterministic model with reserve margin equal to 0.7 are distributed between 422 to 458 thousand dollars which is not very high or low. On average, the expected daily average cost of the deterministic optimization model with reserve margin equal to 0.7 is 0.7 percent higher than that of the here and now model, while its sample standard deviation is 61.4 percent larger than that of the here and now model.

Table 14 Expected daily average cost and sample standard deviation for various reserve margins

Problem	$\overline{E^{DR}}(\$)$	$\overline{\sigma^{DR}}(\$)$
0.0	592,122	212,090

| WR_t | 0.1 | 528,116 | 160,260 |
	0.2	483,807	105,987
	0.3	460,046	63,164
	0.4	448,132	35,534
	0.5	442,595	20,233
	0.6	440,278	12,198
	0.7	439,586	8,109
	0.8	439,763	5,392
	0.9	440,653	4,238
	1.0	442,481	3,530
	1.1	445,130	3,333
	1.2	448,006	3,171
	1.3	450,748	3,038
WR from Jin 2014		448,424	36,893
WS		434,833	5,434
HN		436,391	5,024
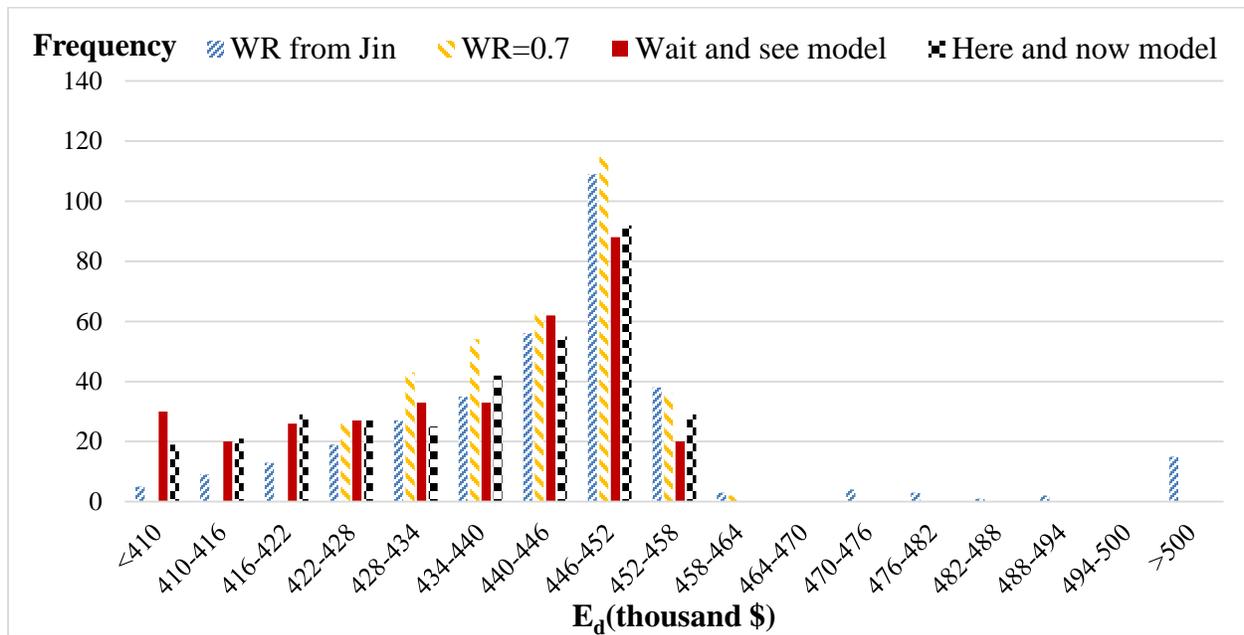
**Figure 29 Frequency for daily average cost for the four models**
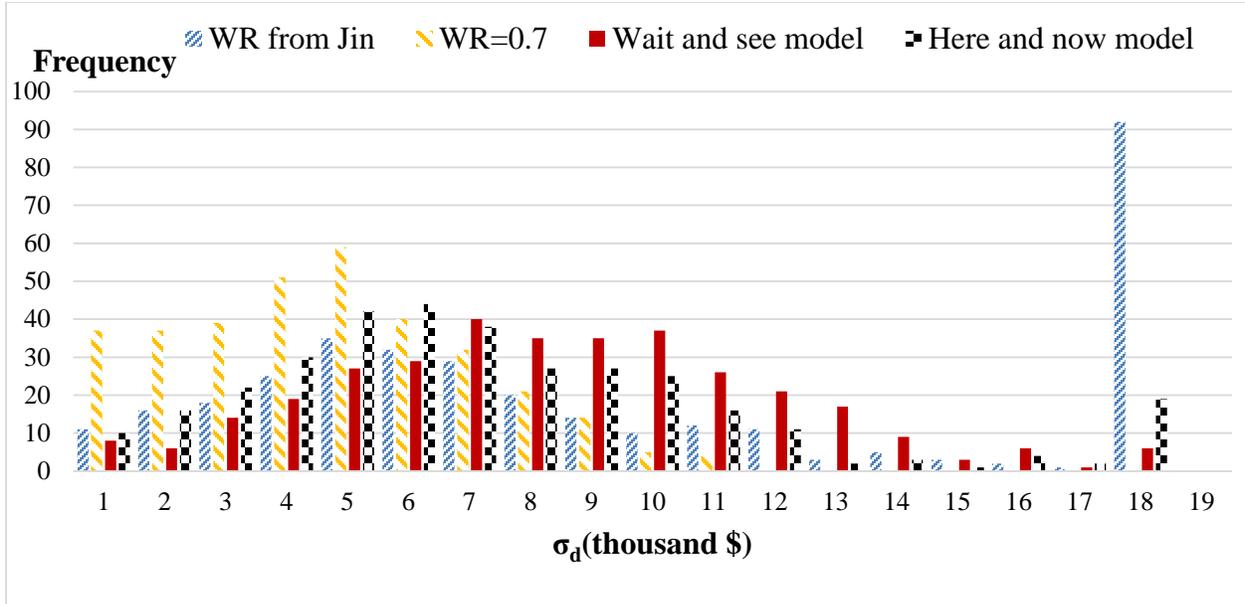
Figure 30 Frequency for daily sample standard deviation for the four models

CHAPTER 7. SUMMARY AND FUTURE RESEARCH

7.1 Summary

In this thesis, three optimization formulations, namely, a deterministic optimization with reserves, a wait and see model and a two-stage stochastic optimization model, are applied to the combined natural gas and electric power system including wind energy to help make the day-ahead decisions on the unit commitment and operation of natural gas pipeline network as well as the real time dispatch and storage facilities' working schedule.

For each day of the 339 days, a one-day case study has been conducted, and the uncertainty of wind energy is assumed. Wind energy scenarios are generated based on quantile regression with a Gaussian copula. Three models are compared in which two are the wait and see and here and now models of the two-stage stochastic optimization model. In the third model, the optimal solution to the deterministic optimization model is obtained with the fixed wind energy prediction and reserve constraints. The results of the here and now model and the deterministic model are compared by fixing the first stage variables to their corresponding optimal solutions and then finding the optimal solution of the second stage variables given various wind energy scenarios.

The experimental result were analyzed and compared to demonstrate that the two-stage planning scheme for the combined system does help to decrease the daily average cost and sample standard deviation of daily cost. Furthermore, the two-stage stochastic optimization model will result in a relevant stable cost given various scenarios compared with the deterministic model.

7.2 Future Research

7.2.1 Assumptions and constraints

In the case study, we assume the start-up cost and shut-down cost of gas power fueled generators are zero and the compressors' operational cost is ignored. In the future study, a more realistic model can be applied based on the real start-up cost and shut-down cost for each gas fueled power generator, the nonlinear expression of the compressors' operational cost and the gas flow through the compressors.

On calculating the amount of gas the gas fueled power generators consume to produce electricity aspect, a more accurate quadratic function of power output would be applied to describe the gas consumption amount, while in this thesis we assume gas consumption amount is a linear function of power output.

The maximum storage flow into or out of the storage faculties depends on the current storage level of the storage facilities, while in this thesis we assume a constant maximum flow value.

7.2.2 Uncertainties

Apart from the wind energy output, more uncertainties should not be left out of the future research work.

We make the first stage decisions one day ahead of the real time market on the basis of some prediction of electric load and non-electric gas demand. However, similar to the wind energy prediction, we cannot assure that all those predictions are exactly accurate and some forecast errors must exist for those two types of parameters. Thus in the future research, it would be a good idea to do some analysis on the electric load and non-electric gas demand forecast and

forecast error, and some scenarios for those two parameters should be generated for the stochastic optimization model analysis.

The non-electric gas demand is assumed to be constant for each hour, and both the non-electric gas demand and the electric load are assumed to be divided into some nodes in the natural gas system or the power system with a constant ratio. In other words, both the non-electric gas demand for each gas node and the electric load in each power system are assumed to increase with the same ratio, but in the practical case, these two parameters depend on many factors, such as season, weather, date, time and temperature. Thus it would be better if we could consider the non-electric gas demand and electric load independently for each node.

Lastly but not the least, the electric power system is designed to be able to work normally even when outages happen to one transmission line or power generator. So in order to have a stable and reliable system operation scheme, incorporating the contingency analysis and post-contingency operation analysis is requisite.

7.2.3 Methodologies

In this thesis, the stochastic optimization model is formulated as a two-stage optimization model. In the future study, more stages could be considered. One simple way is to divide those twenty-four hours of one day into six stages where each stage has four hours. Another modeling methodology is to divide those twenty-hours according to the high peak, medium and low electric load hours. And then we can solve this multi-stage stochastic programming problem and compare the optimal solution with the two-stage stochastic optimization model to study the value of the multi-stage stochastic programming.

In addition to the development of the model itself, more studies could be done to focus on improving the computational efficiency. We test a six-bus power with seven-node gas system which is a quite small case compared with the real case in industry. So the corresponding algorithms for mixed integer stochastic programming, such as progressive hedging algorithm and integer L-shaped method, can be applied to help alleviate the computational burden.

Once we take those nonlinear constraints about the compressors and storage facilities into consideration, the problem would be nonlinear and nonconvex, and the Bender's decomposition could be applied to solve the nonlinear optimization problem.

BIBLIOGRAPHY

Anderson, D. and Leach, M. (2004). Harvesting and redistributing renewable energy: on the role of gas and electricity grids to overcome intermittency through the generation and storage of hydrogen. *Energy Policy*, 32(4):1603-1614.

Barth R., Söder L., Weber C., Brand H., and Swider D. J. (2006). Methodology of the Scenario Tree Tool Tech. Rep. D6.2 (d), Jan. 2006 [Online]. Available: http://www.wilmar.risoe.dk/Results.htm

Bayindir, O., Lu, Y. and Jiang, J.N. (2013). A comparison between perfectly and imperfectly competitive downstream electricity markets under the effect of upstream fuel market price. 2013 8th International Conference on Electrical and Electronics Engineering (ELECO), Bursa, Turkey, Nov. 28th-30th, 2013.

Chaczykowski, M. (2010). Transient flow in natural gas pipeline – The effect of pipeline thermal model. *Applied Mathematical Modelling*, 34(4):1051-1067.

Chen, Y.H. (2014). Theory of the competitive firm. Class notes, EE458, Iowa State University.

Coelho, P.M. and Pinho, C. (2007). Considerations about equations for steady state flow in natural gas pipelines. *Journal of the Brazilian Society of Mechanical Sciences and Engineering*, 29(3):262-273.

Correa-Posada, C.M. and Sanchez-Martin, P. (2013). Stochastic contingency analysis for the unit commitment with natural gas constraints. 2013 IEEE Grenoble Power Tech Conference, France. Jun 16th-20th, 2013

Correa-Posada, C.M. and Sanchez-Martin, P. (2014a). Gas network optimization: A Comparison of piecewise linear models, 2014 [Online]. Available: http://www.optimizationonline.org/DB_HTML/2014/10/4580.htm.

Correa-Posada, C.M. and Sanchez-Martin, P. (2014b). Integrated power and natural gas model for energy adequacy in short-term operation. *IEEE Transactions on Power Systems.* DOI: 10.1109/TPWRS.2014.2372013

Correa-Posada, C.M. and Sanchez-Martin, P. (2014c). Security-constrained optimal power and natural-gas flow. *IEEE Transactions on Power Systems*, 29(4):1780-1787.

DTE Energy (2015). Natural gas processing, delivery and storage. Available: https://www2.dteenergy.com.

Dorin, B. C. and D. Toma-Leonida (2008). On modelling and simulating natural gas transmission systems (part i). *Journal of Control Engineering and Applied Informatics*, 10(23):27–36.

Erdener, B.C., Pambour, K. A., Lavin, R. B. and Dengiz, B (2014). An integrated simulation model for analyzing electricity and gas systems. *International Journal of Electrical Power & Energy Systems*, 61:410-420.

Herrán-González, A, De La Cruz, J.M., De Andrés-Toro, B. and Risco-Martín, J.L. (2009). Modeling and simulation of a gas distribution pipeline network. *Applied Mathematical Modelling*, 33(3):1584-1600.

Høyland, K. and S. W. Wallace (2001). Generating scenario trees for multistage decision problems. *Management Science*, 47(2): 294-307.

Jin, S., Botterud, A. and Ryan, S.M. (2014). Temporal versus stochastic granularity in thermal generation capacity planning with wind power. IEEE Transactions on Power Systems, 29(5):2033-2041.

Kaut M, Wallace SW (2007). Evaluation of scenario-generation methods for stochastic programming. *Pacific Journal of Optimization*, 3(2):257-271.

Li, T., Eremia, M. and Shahidehpour, M. (2008). Interdependency of natural gas network and power system security. *IEEE Transactions on Power Systems*, 23(4):1817-1824.

Liu, C., Shahidehpour, M., Fu, Y. and Li, Z. (2009). Security-constrained unit commitment with natural gas transmission constraints. *IEEE Transactions on Power Systems,* 24(3):1523-1536.

Liu, C., Shahidehpour, M., and Wang, J. (2011). Coordinated scheduling of electricity and natural gas infrastructures with a transient model for natural gas flow. *Chaos: An Interdisciplinary Journal of Nonlinear Science* 21, 2, p025102. DOI: 10.1063/1.3600761.

Lurie PM, Goldberg MS (1998). An approximate method for sampling correlated random variables from partially-specified distributions. *Management Science*, 44(2):203-18.

Macmillan, S., Antonyuk, A. and Schwind, H. (2013). Gas to Coal Competition in the U.S. Power Sector. *International Energy Agency Insights Series 2013*.

Mohitpout, M., Golshan, H. and Murray, A. (2003). Pipeline design and construction: A practical approach, second edition. *The American Society of Mechanical Engineers.*

Morales-España, G., Latorre, J.M. and Ramos, A. (2013). Tight and compact MILP formulation of start-up and shut-down ramping in unit commitment. *IEEE Transactions on Power Systems*, 28(2): 1288 – 1296.

Nico. K. (2012). Gas balancing and line-pack flexibility: concepts and methodologies for organizing and regulating gas balancing in liberalized and integrated EU gas markets (Doctoral dissertation). University of Leuven. Retrieved from https://www.mech.kuleuven.be/en/tme/research/energy_environment/Pdf/wpen2012-11.pdf.

Pflug, G. Ch. (2001). Scenario tree generation for multi-period financial optimization by optimal discretization. *Mathematical Programming*, 89(2): 251-271.

Pinson, P., Madsen, H., Nielsen, A. H., Papaefthymiou, G. and Klockl, B. (2009). From probabilistic forecasts to statistical scenarios of short-term wind power production. *Wind Energy*, 12(1):51-62.

Sari, D., Lee, Y., Ryan, S., Woodruff, D. (2015). Statistical metrics for assessing the quality of wind-power scenarios for stochastic unit commitment. *Wind Energy.* DOI: 10.1002/WC.1872

Shahidehpour, M., Yong, F., Wiedman, T. (2005). Impact of natural gas infrastructure on electric power systems. *Proceedings of the IEEE*, 93(5):1042-1056.

Thompson, M., Davison, M., Rasmussen, H. (2009). Natural gas storage valuation and optimization: A real options application. *Naval Research Logistics*, 56(3): 226-238.

Thorley, A.R.D, Tiley, C.H. (1987). Unsteady and transient flow of compressible fluids in pipelines—a review of theoretical and some experimental studies. *International Journal of Heat and Fluid Flow,* 8(1):3-15.

Unsihuay, C., Marangon-Lima, J.W. and de Souza, A.C.Z. (2007). Short-term operation planning of integrated hydrothermal and natural gas systems. 2007 IEEE Lausanne Power Tech Conference, Lausanne, Switzerland. Jul. 1st-5th, 2007.

Urbina, M. and Li, Z. (2007). A Combined model for analyzing the interdependency of electrical and gas systems. 2007 39th North American Power Symposium. Sep. 30-Oct. 2, 2007. 468-472.

U.S. Energy Information Administration (2014a). Natural gas explained. http://www.eia.gov/energyexplained/index.cfm?page=natural_gas_delivery.

U.S. Energy Information Administration (2014b). U.S. crude oil and natural gas proved reserves, 2013. http://www.eia.gov/naturalgas/crudeoilreserves/pdf/uscrudeoil.pdf.

U.S. Energy Information Administration (2015a). Annual energy outlook 2015 with projections to 2040. http://www.eia.gov/forecasts/aeo/pdf/0383%282015%29.pdf.

U.S. Energy Information Administration (2015b). Natural gas annual 2013. http://www.eia.gov/naturalgas/annual/pdf/nga13.pdf.

U.S. Federal Energy Regulation Commission (2014). Gas-electric coordination quarterly report to the commission. https://www.ferc.gov/legal/staff-reports/2014/12-18-14-gas-electric-cord-quarterly.pdf.

Wu, S., Ríos-Mercado, R.Z., Boyd, E.A. and Scott, L.R. (2000). Model relaxations for the fuel cost minimization of steady-state gas pipeline networks. *Mathematical and Computer Modeling*, 31(2-3):197-220.

Wolf, D.D. and Smeers, Y. (1999). The gas transmission problem solved by an extension of the simplex algorithm. *Management Science*, 46(11):1454-1465.

APPENDIX

A.1 Combined deterministic MILP model

$$
Min\left\{
\begin{array}{l}
\sum_{t=1}^{24}\left[\sum_{ug\in UG}C_{ug}^{SU}su_{ug,t} + \sum_{ug\in UG}C_{ug}^{SD}sd_{ug,t} + \sum_{i\in I}C_i^{NSP}nsp_{i,t} + \sum_{j\in J}C_j^{NSG}nsg_{j,t} + \sum_{stor\in STOR}C_{stor,t}^{STOR}q_{stor,t}^{OUT}\right] \\
+ \sum_{w\in W}C_w^G gp_w + \sum_{t=1}^{24}C^{NSR}nsr_t
\end{array}
\right\}
$$

s.t.

Power flow equilibrium :

$$\sum_{ug\in UG(i)}gpp_{ug,t} + nsp_{i,t} + \sum_{uw\in UW(i)}wpp_{uw,t} \geq PD_{i,t}^{pred} + \sum_{ip\in c_I(i)}pf_{ik,t} \qquad \forall i\in I, \forall t\in T$$

Power startup constraint :

$$u_{ug,t} - u_{ug,t-1} = su_{ug,t} - sd_{ug,t-1} \qquad\qquad \forall ug\in UG, \forall t\in\{2,3,...,24\}$$

$$u_{ug,1} - U_{ug}^{initial} = su_{ug,1} - SD_{ug}^{initial} \qquad\qquad \forall ug\in UG$$

$$u_{ug,t} \geq su_{ug,t} \qquad\qquad \forall ug\in UG, \forall t\in T$$

$$u_{ug,t} \leq 1 - sd_{ug,t} \qquad\qquad \forall ug\in UG, \forall t\in T$$

$$su_{ug,t} + sd_{ug,t} \leq 1 \qquad\qquad \forall ug\in UG, \forall t\in T$$

Maximum & minimum generation :

$$0 \leq gpp_{ug,t} + r_{ug,t} \leq \overline{GPP_{ug}}u_{ug,t} - (\overline{GPP_{ug}} - \underline{GPP_{ug}})su_{ug,t} - (\overline{GPP_{ug}} - \underline{GPP_{ug}})sd_{ug,t} \qquad \forall ug\in UG, \forall t\in T$$

$$gpp_{ug,t} \geq \underline{GPP_{ug}}u_{ug,t} - \underline{GPP_{ug}}su_{ug,t} - \underline{GPP_{ug}}sd_{ug,t} \qquad \forall ug\in UG, \forall t\in T$$

Reserve limit :

$$r_{ug,t} \leq \left[\overline{GPP_{ug}}u_{ug,t} - (\overline{GPP_{ug}} - \underline{GPP_{ug}})su_{ug,t} - (\overline{GPP_{ug}} - \underline{GPP_{ug}})sd_{ug,t}\right]MAXSP_{ug} \qquad \forall ug\in UG, \forall t\in T$$

$$\sum_{ug\in UG}r_{ug,t} + nsr_t \geq WR_t\sum_{uw\in UW}\overline{WPP_{uw,t}} \qquad\qquad \forall t\in T$$

Ramp up and down :

$$-RD_{ug} \leq gpp_{ug,t} - gpp_{ug,t-1} \leq RU_{ug} \qquad\qquad \forall ug\in UG, \forall t\in\{2,3,...,24\}$$

$$-RD_{ug} \leq gpp_{ug,1} - GPP_{ug}^{initial} \leq RU_{ug} \qquad\qquad \forall ug\in UG$$

Minimum on and off time :

$$\sum_{tt=t-TU_{ug}+1}^{t} su_{ug,t} \le u_{ug,t} \qquad\qquad \forall ug \in UG, \forall t \in \{TU_{ug},\ldots,24\}$$

$$\sum_{tt=t-TD_{ug}+1}^{t} sd_{ug,t} \le 1-u_{ug,t} \qquad\qquad \forall ug \in UG, \forall t \in \{TD_{ug},\ldots,24\}$$

Wind power capacity :

$$wpp_{uw,t} \le \overline{WPP_{uw,t}} \qquad\qquad \forall uw \in UW, \forall t \in T$$

Transmission line constraint :

$$pf_{i,ip,t} = \frac{\theta_{i,t} - \theta_{ip,t}}{X_{i,ip}} \qquad\qquad \forall ip \in c_I(i), \forall i \in I$$

$$-\overline{PF_{i,ip,t}} \le pf_{i,ip,t} \le \overline{PF_{i,ip,t}} \qquad\qquad \forall ip \in c_I(i), \forall i \in I$$

Gas flow equilibrium :

$$\sum_{w\in W(j)} \frac{gp_w}{24} + \sum_{stor \in STOR(j)} \left(q_{stor,t}^{OUT} - q_{stor,t}^{IN}\right) + nsg_{j,t} \ge PD_{i,t}^{pred} + \sum_{ug \in UG(j)} egd_{ug,t} + \sum_{jp \in c_J(j)} gf_{jp,j,t} \qquad \forall j \in J, t \in T$$

$$\underline{GP_w} \le gp_w \le \overline{GP_w} \qquad\qquad \forall w \in W$$

Gas storage flow :

$$\underline{Cap_{stor}} \le level_{stor,t} \le \overline{Cap_{stor}} \qquad\qquad \forall stor \in STOR, \forall t \in T$$

$$level_{stor,t} = level_{stor,t-1} - q_{stor,t}^{OUT} + q_{stor,t}^{IN} \qquad\qquad \forall stor \in STOR, \forall t \in \{2,3,4,\ldots,24\}$$

$$level_{stor,t-1} - \overline{Cap_{stor}} \le q_{stor,t}^{OUT} - q_{stor,t}^{IN} \le level_{stor,t-1} - \underline{Cap_{stor}} \qquad\qquad \forall stor \in STOR, \forall t \in \{2,3,4,\ldots,24\}$$

$$-Q_{stor} \le q_{stor,t}^{OUT} - q_{stor,t}^{IN} \le Q_{stor} \qquad\qquad \forall stor \in STOR, \forall t \in T$$

Gas flow in pipeline :

$$\pi_{j,t} = \left(pr_{j,t}\right)^2 \qquad\qquad \forall j \in J, \forall t \in T$$

$$\Delta\pi_{j,jp,t} = \pi_{j,t} - \pi_{jp,t} \qquad\qquad \forall jp \in c_J(j), \forall j \in J, \forall t \in T$$

$$\Delta\pi_{j,jp,t} = \Delta\pi_{j,jp,t}^{1} + \sum_{p_{j,jp}\in P} (\Delta\pi_{j,jp,t}^{p_{j,jp}+1} - \Delta\pi_{j,jp,t}^{p_{j,jp}})\delta_{j,jp,t}^{p_{j,jp}} \qquad\qquad \forall jp \in c_J(j), \forall j \in J, \forall t \in T$$

$$gf_{j,jp,t} = GF_{j,jp,t}^{1} + \sum_{p_{j,jp}\in P} (GF_{j,jp,t}^{p_{j,jp}+1} - GF_{j,jp,t}^{p_{j,jp}})\delta_{j,jp,t}^{p_{j,jp}} \qquad\qquad \forall jp \in c_J(j), \forall j \in J, \forall t \in T$$

$$GF_{j,jp,t}^{p_{j,jp}} = sgn(\Delta\pi_{j,jp,t}^{p_{j,jp}})C_{j,jp}\sqrt{|\Delta\pi_{j,jp,t}^{p_{j,jp}}|} \qquad\qquad \forall jp \in c_J(j), \forall j \in J, \forall t \in T$$

$$\delta_{j,jp,t}^{p_{j,jp}+1} \le y_{j,jp,t}^{p_{j,jp}} \le \delta_{j,jp,t}^{p_{j,jp}} \qquad\qquad \forall p_{j,jp} \in P-1$$

$$0 \le \delta_{j,jp,t}^{p_{j,jp}} \le 1 \qquad\qquad \forall p_{j,jp} \in P$$

Active pipeline constraints :

$$gf_{j,ajp,t} = \text{sgn}(pr_{j,t} - pr_{j,ajp,t}^{left})C_{j,ajp,t}^{left}\sqrt{\left|\left(pr_{p,ajp,t}^{left}\right)^2 - \left(pr_{j,t}\right)^2\right|} \qquad \forall pr_{p,ajp,t}^{left} \in c_J^{AP}(j)$$

$$gf_{j,ajp,t} = \text{sgn}(pr_{j,ajp,t}^{right} - pr_{ajp,t})C_{j,ajp,t}^{right}\sqrt{\left|\left(pr_{p,ajp,t}^{right}\right)^2 - \left(pr_{jp,t}\right)^2\right|} \qquad \forall pr_{jp,t} \in c_J^{AP}(j)$$

$$\frac{pr_{j,jp,,t}^{right}}{\tau_{j,ajp}} \le pr_{j,ajp,t}^{left} \le pr_{j,ajp,t}^{right}\tau_{j,ajp} \qquad \forall ajp \in c_J^{A}(j)$$

Connection :

$$egd_{ug,t} = Bf_{ug}\left(gpp_{ug,t} + r_{ug,t}\right) + Cf_{ug} \qquad \forall ug \in UG, \forall t \in T$$

$$u_{ug,t}, su_{ug,t}, sd_{ug,t} \in \{0,1\} \qquad \forall ug \in UG, \forall t \in T$$

$$y_{j,jp,t}^{p_{j,jp}} \in \{0,1\} \qquad \forall jp \in c_J(j), \forall j \in J, \forall t \in T$$

$$gpp_{ug,t}, r_{ug,t}, egd_{ug,t} \ge 0 \qquad \forall ug \in UG, \forall t \in T$$

$$nsp_{i,t} \ge 0 \qquad \forall i \in I, \forall t \in T$$

$$wpp_{uw,t} \ge 0 \qquad \forall uw \in UW, \forall t \in T$$

$$nsr_t \ge 0 \qquad \forall t \in T$$

$$gp_w \ge 0 \qquad \forall w \in W, \forall t \in T$$

$$nsg_{j,t}, \pi_{j,t}, pr_{j,t} \ge 0 \qquad \forall j \in J, \forall t \in T$$

$$pr_{j,ajp,t}^{left}, pr_{j,ajp,t}^{right} \ge 0 \qquad \forall ajp \in c_J^{A}(j)$$

$$\delta_{j,jp,t}^{p_{j,jp}} \ge 0 \qquad \forall jp \in c_J(j), \forall j \in J, \forall t \in T$$

$$level_{stor,t}, q_{stor,t}^{OUT}, q_{stor,t}^{IN} \ge 0 \qquad \forall stor \in STOR, \forall t \in T$$

A.2 Combined stochastic here and now model MILP model

$$Min\left\{\sum_{w\in W} C_w^G \, gp_w + \sum_{t=1}^{24} \sum_{ug\in UG}\left[C_{ug}^{SU} su_{ug,t} + C_{ug}^{SD} sd_{ug,t}\right] + \varphi\right\}$$

s.t.

$$\underline{GP_w} \le gp_w \le \overline{GP_w} \qquad\qquad\qquad \forall w \in W$$

Power startup constraint :

$$u_{ug,t} - u_{ug,t-1} = su_{ug,t} - sd_{ug,t-1} \qquad\qquad \forall ug \in UG, \forall t \in \{2,3,...,24\}$$

$$u_{ug,1} - U_{ug}^{initial} = su_{ug,1} - SD_{ug}^{initial} \qquad\qquad \forall ug \in UG$$

$$u_{ug,t} \ge su_{ug,t} \qquad\qquad \forall ug \in UG, \forall t \in T$$

$$u_{ug,t} \le 1 - sd_{ug,t} \qquad\qquad \forall ug \in UG, \forall t \in T$$

$$su_{ug,t} + sd_{ug,t} \le 1 \qquad\qquad \forall ug \in UG, \forall t \in T$$

Minium on and off time :

$$\sum_{tt=t-TU_{ug}+1}^{t} su_{ug,t} \le u_{ug,t} \qquad\qquad \forall ug \in UG, \forall t \in T$$

$$\sum_{tt=t-TD_{ug}+1}^{t} sd_{ug,t} \le 1 - u_{ug,t} \qquad\qquad \forall ug \in UG, \forall t \in T$$

$$\Delta\pi_{j,jp,t} = \pi_{j,t} - \pi_{jp,t} \qquad\qquad \forall jp \in c_J(j), \forall t \in T$$

$$\Delta\pi_{j,jp,t} = \Delta\pi_{j,jp,t}^1 + \sum_{p_{j,jp}\in P}(\Delta\pi_{j,jp,t}^{p_{j,jp}+1} - \Delta\pi_{j,jp,t}^{p_{j,jp}})\delta_{j,jp}^{p_{j,jp}} \qquad \forall jp \in c_J(j), \forall j \in J, \forall t \in T$$

$$gf_{j,jp,t} = GF_{j,jp,t}^1 + \sum_{p_{j,jp}\in P}(GF_{j,jp,t}^{p_{j,jp}+1} - GF_{j,jp,t}^{p_{j,jp}})\delta_{j,jp}^{p_{j,jp}} \qquad \forall jp \in c_J(j), \forall j \in J, \forall t \in T$$

$$GF_{j,jp,t}^{p_{j,jp}} = sgn(\Delta\pi_{j,jp,,t}^{p_{j,jp}})C_{j,jp}\sqrt{|\,\Delta\pi_{j,jp,t}^{p_{j,jp}}\,|} \qquad \forall jp \in c_J(j), \forall j \in J, \forall t \in T$$

$$GF_{j,jp,t}^{p_{j,jp}} = sgn(\Delta\pi_{j,jp,,t}^{p_{j,jp}})C_{j,jp}\sqrt{|\,\Delta\pi_{j,jp,t}^{p_{j,jp}}\,|} \qquad \forall jp \in c_J(j), \forall j \in J, \forall t \in T$$

$$\delta_{j,jp}^{p_{j,jp}+1} \le y_{j,jp}^{p_{j,jp}} \le \delta_{j,jp}^{p_{j,jp}} \qquad\qquad \forall p_{j,jp} \in P-1$$

$$0 \le \delta_{j,jp}^{p_{j,jp}} \le 1 \qquad\qquad \forall p_{j,jp} \in P$$

Active pipeline constraints :

$$gf_{j,ajp,t} = sgn(pr_{j,t} - pr_{j,ajp,t}^{left})C_{j,ajp,t}^{left}\sqrt{|\,(pr_{p,ajp,t}^{left})^2 - (pr_{j,t})^2\,|} \qquad \forall pr_{p,ajp,t}^{left} \in c_J^{AP}(j)$$

$$gf_{j,ajp,t} = sgn(pr_{j,ajp,t}^{right} - pr_{ajp,t})C_{j,ajp,t}^{right}\sqrt{|\,(pr_{p,ajp,t}^{right})^2 - (pr_{jp,t})^2\,|} \qquad \forall pr_{jp,t} \in c_J^{AP}(j)$$

$$\frac{pr_{j,jp,,t}^{right}}{\tau_{j,ajp}} \le pr_{j,ajp,t}^{left} \le pr_{j,ajp,t}^{right}\tau_{j,ajp} \qquad\qquad \forall ajp \in c_J^A(j)$$

$$u_{ug,t}, su_{ug,t}, sd_{ug,t} \in \{0,1\} \qquad\qquad \forall ug \in UG, \forall t \in T$$

$$y_{j,jp,t}^{p_j,jp} \in \{0,1\} \qquad\qquad \forall jp \in c_J(j), \forall j \in J, \forall t \in T$$

$$gpp_{ug,t} \geq 0 \qquad\qquad \forall ug \in UG, \forall t \in T$$

$$nsr_t \geq 0 \qquad\qquad \forall t \in T$$

$$gp_w \geq 0 \qquad\qquad \forall w \in W, \forall t \in T$$

$$\pi_{j,t}, pr_{j,t} \geq 0 \qquad\qquad \forall j \in J, \forall t \in T$$

$$pr_{j,ajp,t}^{left}, pr_{j,ajp,t}^{right} \geq 0 \qquad\qquad \forall ajp \in c_J^A(j)$$

$$\delta_{j,jp,t}^{p_j,jp} \geq 0 \qquad\qquad \forall jp \in c_J(j), \forall j \in J, \forall t \in T$$

Wind power capacity :

$$wpp_{uw,t}^s \leq \overline{WPP_{uw,t}^s} \qquad\qquad \forall uw \in UW, \forall t \in T, \forall s \in S$$

$$\varphi = \min\left\{ \sum_{s \in S} prob_s \sum_{t=1}^{24}\left[\sum_{i \in I} C_i^{NSP} nsp_{i,t}^s + \sum_{j \in J} C_j^{NSG} nsg_{j,t}^s + \sum_{stor \in STOR} C_{stor,t}^{STOR} q_{stor,t}^{OUT,s} \right] \right\}$$

s.t.

Maximum & minimum generation :

$$0 \leq gpp_{ug,t}^s \leq \overline{P_{ug}^P} u_{ug,t} - (\overline{P_{ug}^P} - \underline{P_{ug}^P}) su_{ug,t} - (\overline{P_{ug}^P} - \underline{P_{ug}^P}) sd_{ug,t} \qquad \forall ug \in UG, \forall t \in T, \forall s \in S$$

$$gpp_{ug,t}^s \geq \underline{P_{ug}^P} u_{ug,t} - \underline{P_{ug}^P} \times su_{ug,t} - \underline{P_{ug}^P} sd_{ug,t} \qquad \forall ug \in UG, \forall t \in T, \forall s \in S$$

Ramp up and down :

$$-RD_{ug} \leq gpp_{ug,t}^s - gpp_{ug,t-1}^s \leq RU_{ug} \qquad \forall ug \in UG, \forall t \in \{2,3,...,24\}, \forall s \in S$$

$$-RD_{ug} \leq gpp_{ug,1}^s - GPP_{ug}^{initial} \leq RU_{ug} \qquad \forall ug \in UG, \forall s \in S$$

Power flow equilibrium :

$$\sum_{ug \in UG(i)} gpp_{ug,t}^s + nsp_{i,t}^s + \sum_{uw \in UW(i)} wpp_{uw,t}^s \geq PD_{i,t}^{pred} + \sum_{ip \in c_I(i)} pf_{ik,t}^s \qquad \forall i \in I, \forall t \in T, \forall s \in S$$

Transmission line constraint :

$$pf_{i,ip,t}^s = \frac{\theta_{i,t}^s - \theta_{ip,t}^s}{X_{i,ip}} \qquad \forall ip \in c_I(i), \forall i \in I, \forall s \in S$$

$$-\overline{PF_{i,ip,t}} \leq pf_{i,ip,t}^s \leq \overline{PF_{i,ip,t}} \qquad \forall ip \in c_I(i), \forall i \in I, \forall s \in S$$

Gas flow euqilibrium :

$$\sum_{w \in W(j)} \frac{gp_w}{24} + \sum_{stor \in STOR(j)} \left(q_{stor,t}^{OUT,s} - q_{stor,t}^{IN,s} \right) + nsg_{j,t}^s \geq GD_{j,t}^{pred} + \sum_{ug \in UG(j)} egd_{ug,t}^s + \sum_{jp \in c_J(j)} gf_{jp,j,t}^s$$

$$\forall j \in J, t \in T, \forall s \in S$$

Gas storage flow :

$$\underline{Cap_{stor}} \leq level^s_{stor,t} \leq \overline{Cap_{stor}} \qquad \forall stor \in STOR, \forall t \in T, \forall s \in S$$

$$level_{stor,t} = level^s_{stor,t-1} - q^{OUT,s}_{stor,t} + q^{IN,s}_{stor,t} \qquad \forall stor \in STOR, \forall t\{2,3,...,24\}, \forall s \in S$$

$$level^s_{stor,1} = LEVEL^{initial}_{stor} - q^{OUT,s}_{stor,1} + q^{IN,s}_{stor,1} \qquad \forall stor \in STOR, \forall s \in S$$

$$level^s_{stor,t-1} - \overline{Cap_{stor}} \leq q^{OUT,s}_{stor,t} - q^{IN,s}_{stor,t} \leq level^s_{stor,t-1} - \underline{Cap_{stor}} \qquad \forall stor \in STOR, \forall t \in T, \forall s \in S$$

$$-Q_{stor} \leq q^{OUT,s}_{stor,t} - q^{IN,s}_{stor,t} \leq Q_{stor} \qquad \forall stor \in STOR, \forall t \in T, \forall s \in S$$

Connection :

$$egd^s_{ug,t} = Bf_{ug}\, gpp^s_{ug,t} + Cf_{ug} \qquad \forall ug \in UG, \forall t \in T, \forall s \in S$$

$$gpp^s_{ug,t}, egd^s_{ug,t} \geq 0 \qquad \forall ug \in UG, \forall t \in T, \forall s \in S$$

$$nsp^s_{i,t} \geq 0 \qquad \forall i \in I, \forall t \in T, \forall s \in S$$

$$wpp^s_{uw,t} \geq 0 \qquad \forall uw \in UW, \forall t \in T, \forall s \in S$$

$$nsg^s_{j,t} \geq 0 \qquad \forall j \in J, \forall t \in T, \forall s \in S$$

$$q^{OUT,s}_{stor,t}, q^{IN,s}_{stor,t}, level^s_{stor,t} \qquad \forall stor \in STOR, \forall t \in T, \forall s \in S$$